THE IMPACT OF SOME ASPECTS OF THE BOUNDARY LAYER SCHEME IN THE ECMWF MODEL

Anton C.M.Beljaars
(Royal Netherlands Meteorological Institute)

1. Introduction

The atmospheric boundary layer is the lower part of the troposphere where the direct influence from the surface is felt through turbulent exchange with the surface. The impact of the boundary layer in models is particularly felt after a few days of integration when the accumulated surface fluxes contribute substantially to the heat moisture and momentum balance of the atmosphere. The boundary layer also determines the shape of the profiles near the surface and is therefore crucial for near surface parameters as 10 m wind and temperature and humidity at screen level, also in the short range and during data assimilation.

This paper is not a review of recent impact studies (as e.g. Garratt, 1993), but a rather specific account of activities at ECMWF over the last few years. A number of changes to the boundary layer scheme have been tested and some of them have been implemented. In this paper, the results of experimentation with the boundary layer scheme will be discussed as sensitivity experiments. The main conclusion is that changes have impact, when the surface fluxes are affected. However, surface fluxes are not independent of the structure of the boundary layer. If we think of the boundary layer for simplicity as a reservoir (e.g. a mixed layer), of momentum, heat and moisture, then it becomes clear that all processes affecting the contents of the reservoir have impact on the surface fluxes. If for instance the boundary layer is ventilated at the top through dry entrainment or through moist convection, then the boundary layer becomes dryer and the surface evaporation increases (Tiedtke et al. 1988). Also the stable boundary layer has a complicated interaction between its structure and the surface fluxes. The latter is of particular importance for the momentum flux in winter over continental areas.

2. Transfer coefficients over the ocean

Transfer coefficients between the lowest model level and the ocean surface have direct impact on the surface fluxes. The surface flux of moisture is particularly important since it drives the hydrological cycle and it is the dominant energy source of the atmosphere. Two examples of impact are given: (i) the transfer coefficients at low wind speeds affecting the tropical circulation and (ii) the transfer coefficients at high winds which are more important in the extra-tropics.

2.1 Low winds

An important geographical area for the global circulation is the so called warm pool area in the Western Pacific, characterized by high sea surface temperatures and relatively low wind speeds. The convective activity in this area is high, but the advection is limited, so the local evaporation plays a crucial role in determining the convective activity. Fig. 1 illustrates the change to the transfer coefficients that was made in 1990 to the operational ECMWF model. We concentrate on the wind speed range below 5 m/s which shows an increase of the transfer coefficient for moisture by about 30 %. For the latent heat flux at zero wind speed for typical air-sea differences of 1.5 K and 7 g/kg respectively, it implies an increase from 5 to about 40 W/m^2. The increase of the transfer coefficient at low wind speeds is well documented now (Liu et al., 1979; Schumann, 1988; Godfrey and Beljaars, 1991; Beljaars, 1995) and also supported by observations (Bradley et al., 1991). The details of the impact studies that have been made with these changes are given by Miller et al. (1992); here we limit to a short summary.

The main impact is found in the tropics, where the stronger coupling between atmosphere and ocean results in a more intense hydrological cycle with a stronger Hadley cell, more evaporation, more precipitation and reduced wind errors. An example of precipitation results is shown in Fig. 2

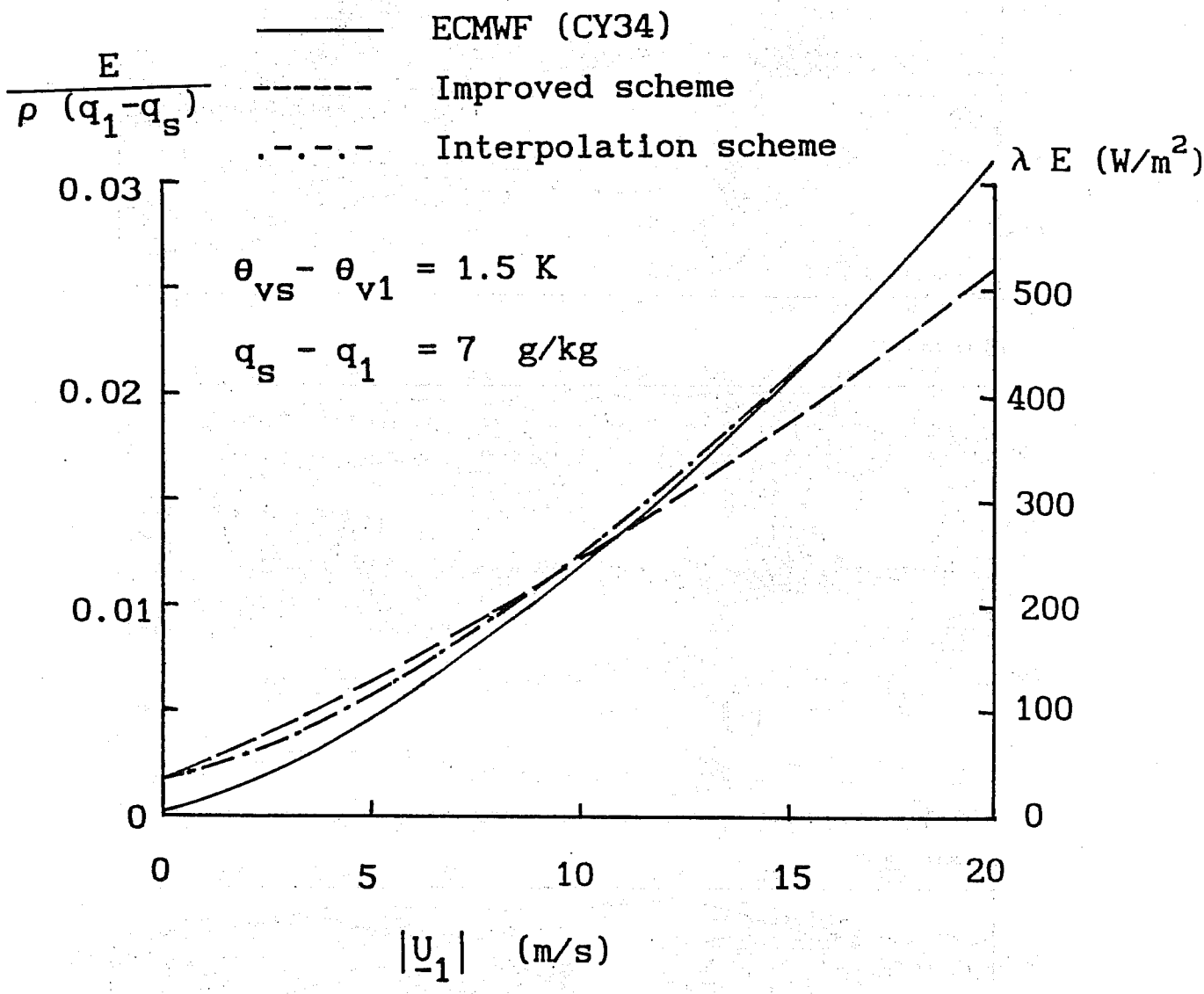

Fig. 1 The "conductivity" of the lowest model layer for moisture transfer as a function of wind speed. The reference height is 32 m, which is the height of the lowest model level in the ECMWF model. The right-hand scale indicates the latent heat flux for a typical temperature difference of 1.5 K and a specific humidity difference of 7 g/kg. The solid line represents the old scheme, the dashed line the preferred new scheme and the dash-dot line the scheme that was implemented in 1990 to limit the effect to low winds.

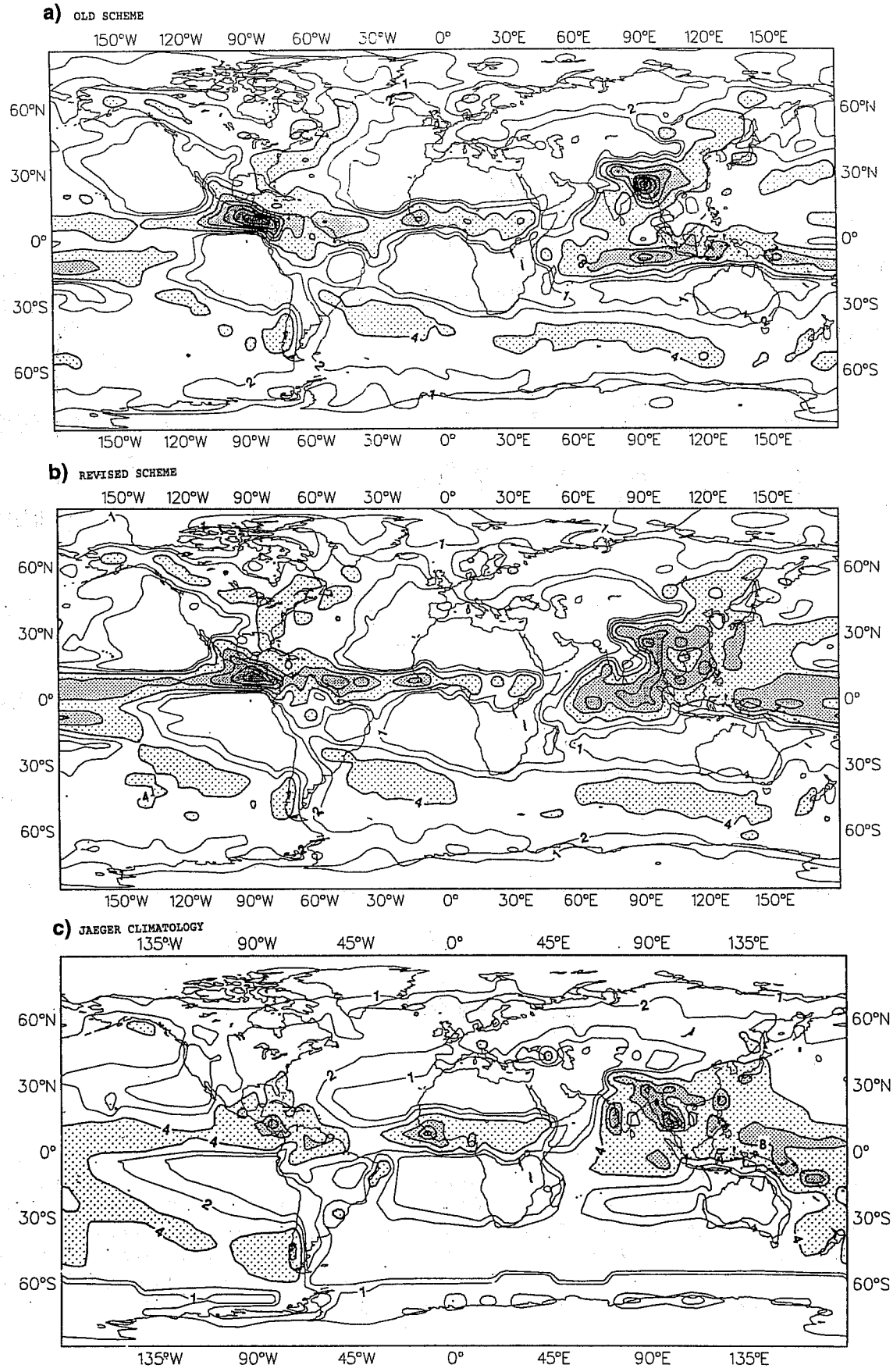

Fig. 2 Rainfall averaged over 90 days of a T42, NH summer experiment. Fig. (A) refers to the old scheme, (B) to the parametrization with the enhanced air-sea coupling at low winds and (C) to climatoly by Jaeger. Contours are at 1,2,4,8 .... mm/day.

from long runs at T42 resolution. The old model has a dry zone over the warm pool in the Western Pacific, which disappears with the new scheme and the Hadley circulation is generally stronger with the new scheme. The evaporation shows a similar picture, with increased evaporation in the trade wind areas (Fig.3). The increased latent heat release in a concentrated ITCZ in the Western Pacific leads to reduced Easterly errors in the upper troposphere as shown in Fig. 4.

This change in the parametrization of evaporation over the tropical oceans was very successful in reducing the systematic bias in the tropical circulation in spite of the relatively small magnitude of the change. It should be realized that the impact is amplified by a positive feedback. With regard to transfer coefficients between atmosphere and ocean we would expect a negative feedback because enhanced coupling reduces the specific humidity difference between atmosphere and ocean. However, the increased strength of the Hadley circulation enhances the surface wind which makes the coupling stronger. It is this positive feedback which makes the tropical circulation so sensitive to to small changes in the parametrization of transfer coefficients.

2.2 High winds

The transfer coefficients at high wind speeds were changed in July 1993 with the introduction of model cycle 48. The change is illustrated in Fig. 5. The old scheme had the Charnock formulation for the sea surface roughness length, which was used for momentum as well as heat and moisture. The heat and moisture flux had an empirical fix for the low wind parametrization (see previous section). For simplicity we consider the following two parametrizations and call them old (nearly cy47) and new (cy48). The roughness lengths in the old scheme are:

$$z_{om} = 0.11\ \nu/u_* + 0.018\ u_*^2/g\ ,$$
$$z_{oh} = 0.40\ \nu/u_* + 0.018\ u_*^2/g\ , \qquad (1)$$
$$z_{oq} = 0.62\ \nu/u_* + 0.018\ u_*^2/g\ ,$$

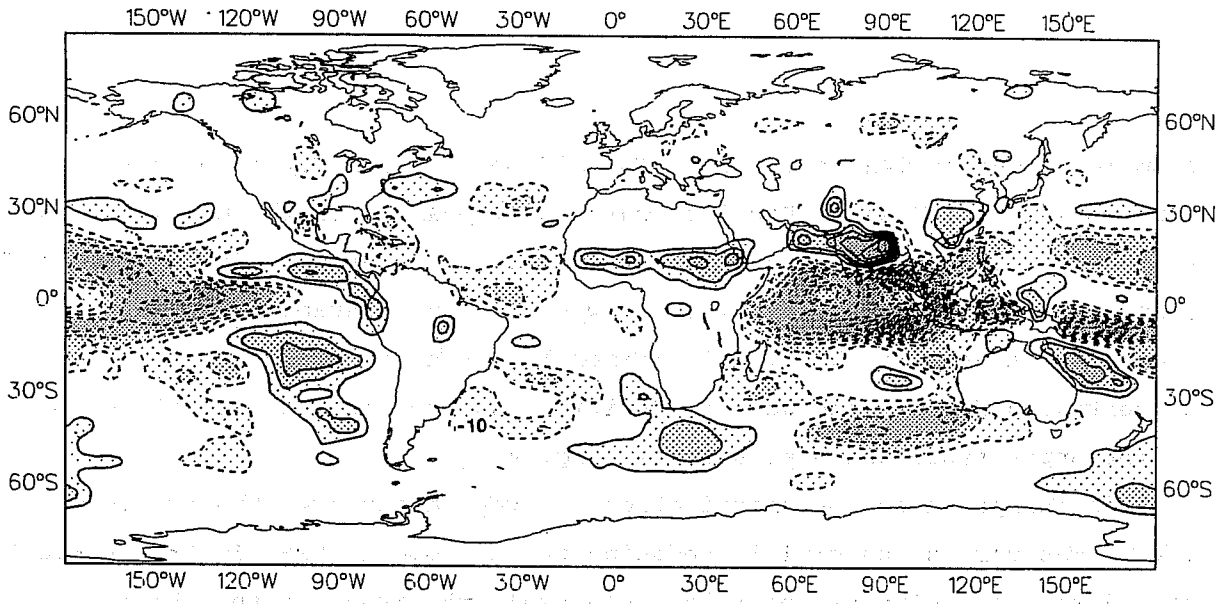

Fig. 3 Evaporation difference between the scheme with enhanced air-sea coupling at low winds and the old parametrization from T42 experiments for June-July-August (90 day average). Negative values indicate an increase in evaporation (downward fluxes are positive by model convention) and have dashed contours. The contour interval is 10 W/m^2.

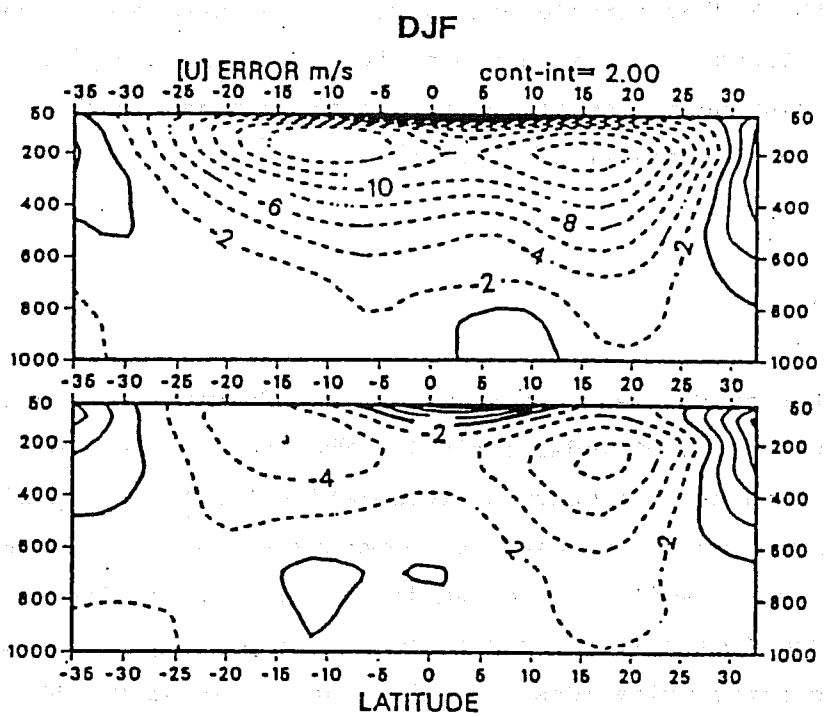

Fig. 4 Zonal mean wind errors (difference between model and analysis) averaged over 90 days for December-January-February T42 integrations with the old scheme (upper panel) and the scheme with enhanced air-sea coupling (lower panel).

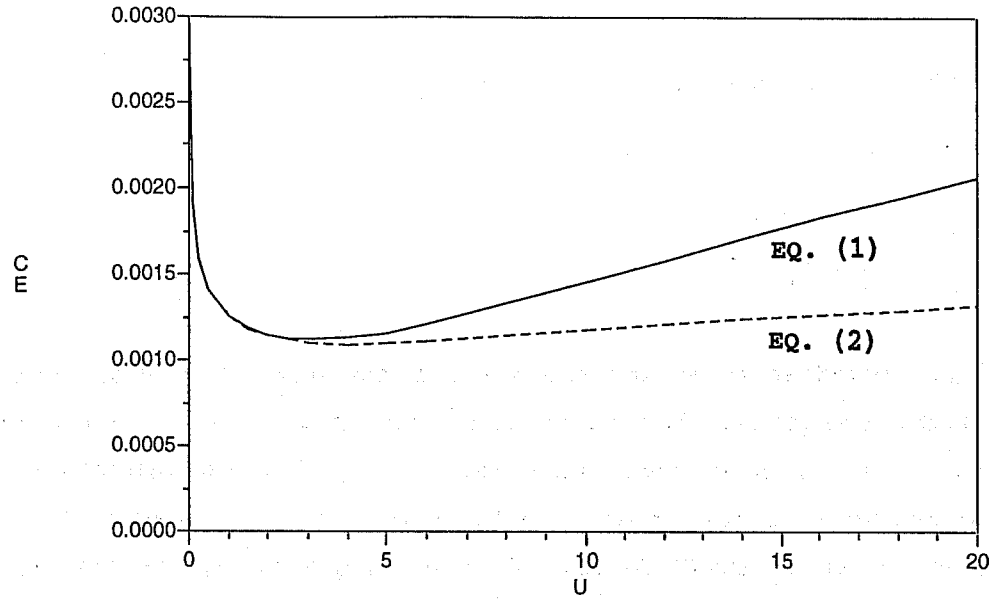

Fig. 5 Neutral air-sea transfer coefficients for water vapor (reference level 10 m) according to equation (1) as in model cycle 47 and according to equation (2) as in model cycle 48.

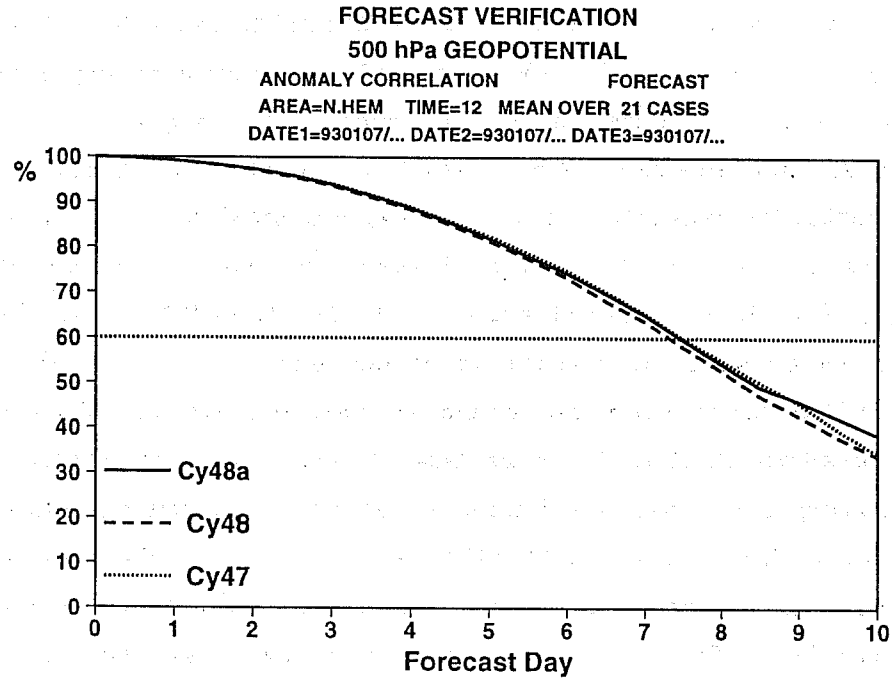

Fig. 6 500 hPa anomaly correlation for the Northern Hemisphere averaged over 21 forecasts with three forecast systems (full data assimilation/ forecast systems are compared here for January 1993) at T106L31 resolution. The dotted line is with cycle 47, the dashed line is with cycle 48, and the solid line is with cycle 48 and the air-sea interaction reverted to cycle 47.

and for the new parametrization (cy48):

$$z_{om} = 0.11\ \nu/u_* + 0.018\ u_*^2/g$$
$$z_{oh} = 0.40\ \nu/u_* \qquad (2)$$
$$z_{oq} = 0.62\ \nu/u_*$$

The old parametrization is not the exact formulation of the operational model before the change, but it is reasonably close and it is the one that was used for sensitivity tests afterwards. From forecast experiments with this change, very little impact was found in general. However, the re-analysis group at ECMWF found a distinct negative impact from cycle 48 with respect to cycle 47 for the January 1993 period (see objective scores for the Northern Hemisphere in Fig. 6) from a data assimilation experiment with forecasts over 21 days. From additional experimentation it became clear that reverting to the cycle 47 air-sea interaction, also gave the cycle 47 objective scores for this period. It was therefore concluded that the reduced air-sea coupling had a negative impact on the model performance for this particular period. It should be emphasized that this result can not be generalized; earlier data-assimilation-forecast experiments had shown positive or neutral impact for cycle 48. The question remains why the revised air-sea interaction has negative impact for January 1993, in spite of the better representation of the experimental data on transfer coefficients. DeCosmo (1991) for instance reports a constant value of the transfer coefficient for moisture of 0.0012 from HEXOS data, which is in good agreement with the results from equation (2) in Fig. 5.

The effect of the air-sea transfer coefficients for the January 1993 period is shown in Fig. 7, where the 24 hour latent heat flux difference is shown averaged over all 21 forecasts. There is a clear increase of the latent heat fluxes over the North-West Atlantic and the North-West Pacific with the enhanced transfer coefficients at high winds. These are the areas with cold air outflow over relatively warm water, which is a particularly dominant feature for January. The results so far suggest that the increased evaporation in the areas with cold air outflow, is related to the improvement of the objective scores in the medium range. On the other hand we know that the new transfer coefficients give a better fit of the

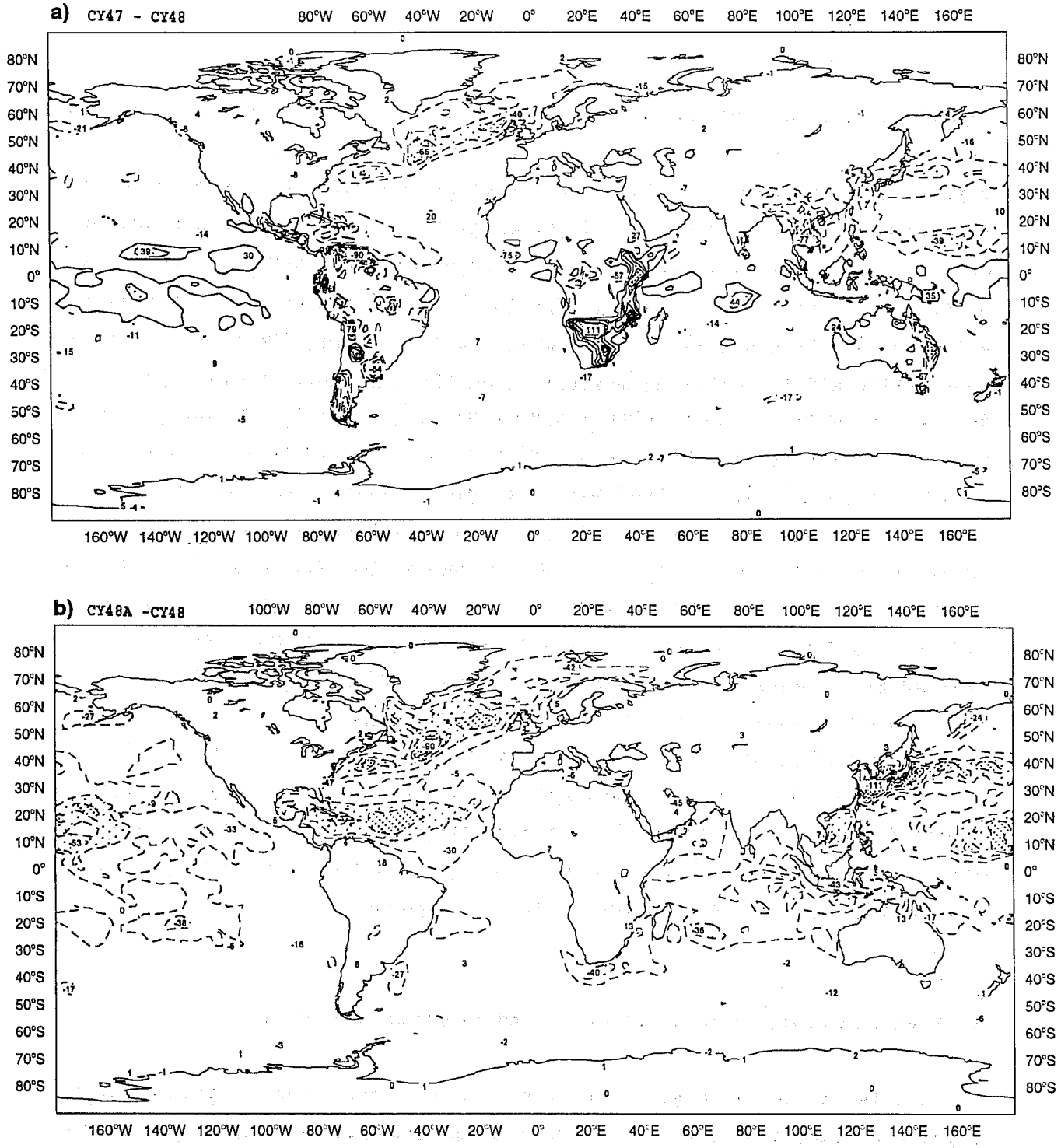

Fig. 7 The difference in latent heat flux between cycle 47 and cycle 48 (A) and the difference between cycle 48 with air-sea interaction reverted to cycle 47 and cycle 48 (B). The 24 hour accumulated values are averaged over 21 forecasts initialized from their own analysis (January 1993).

experimental data (DeCosmo, 1991). Consequently it can be expected that too high transfer coefficients compensate for another deficiency in the model. This is believed to be the too moist state of the model troposphere which is evident from the comparison of the model first guesses with radiosondes over the North Atlantic (Fig. 8). So it appears that other processes in the model are not efficient enough in drying the model atmosphere. A possible candidate is the convection scheme which is responsible for boundary layer ventilation and for deleting moisture from the atmosphere by precipitation. Because the model atmosphere is systematically too moist, we conjecture that the convection scheme is not active enough. To increase the convection activity particularly in areas with cold air outflow it was tried to include the surface sensible heat flux in addition to the latent heat flux in the closure of the shallow convection scheme. The effect of this change on the surface latent heat flux is shown in Fig. 9 in comparison with the effect of enhanced air-sea interaction coefficients. We sea clear similarities, which are due to drying of the model atmosphere which enhances evaporation. This is also evident from the fit to the radiosonde relative humidity data (see Fig. 8) and the objective scores (Fig. 10).

We conclude from this example that the unrealistically high transfer coefficients in model cycle 47 were compensating a moist bias over areas with cold air advection. The cause of the moist bias is not certain, but very likely related to an underactivity of convection.

3. Thermodynamic structure of the boundary layer over land

In this section we discuss the thermodynamic structure of the boundary layer over land in relation to fluxes at the surface and fluxes at the top of the boundary layer. Two aspects are distinguished namely the warm bias over summer continents and the diurnal cycle of near surface parameters.

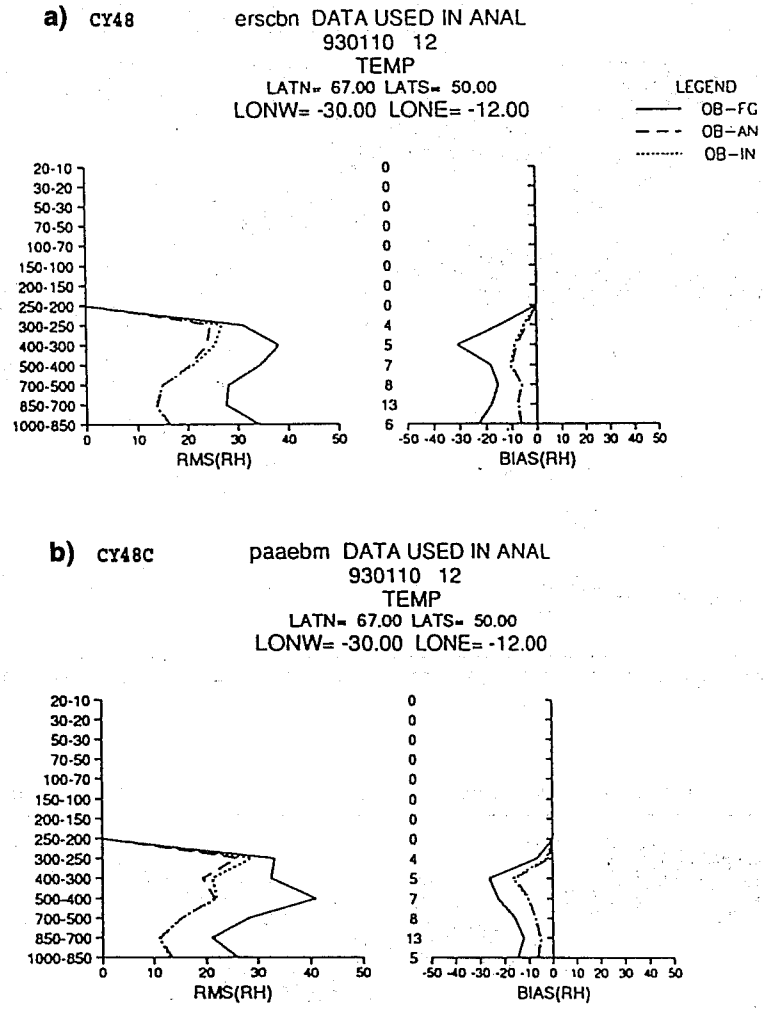

Fig. 8 Analysis statistics of 12 UTC relative humidity, averaged over sonde stations of the North Atlantic (between 50°-67° and 30°-12°W) and over 5 days of data assimilation for January 1993. The solid line refers to the first guess (observation - 6 hour forecasts), the dashed and the dotted line refer to the analysis and initialized analysis respectively. The left hand figures shows the RMS difference between sonde and model, the right hand figure shows the bias. Fig. A refers to cycle 48, Fig. B refers to cycle 48 with revised closure of the shallow convection scheme.

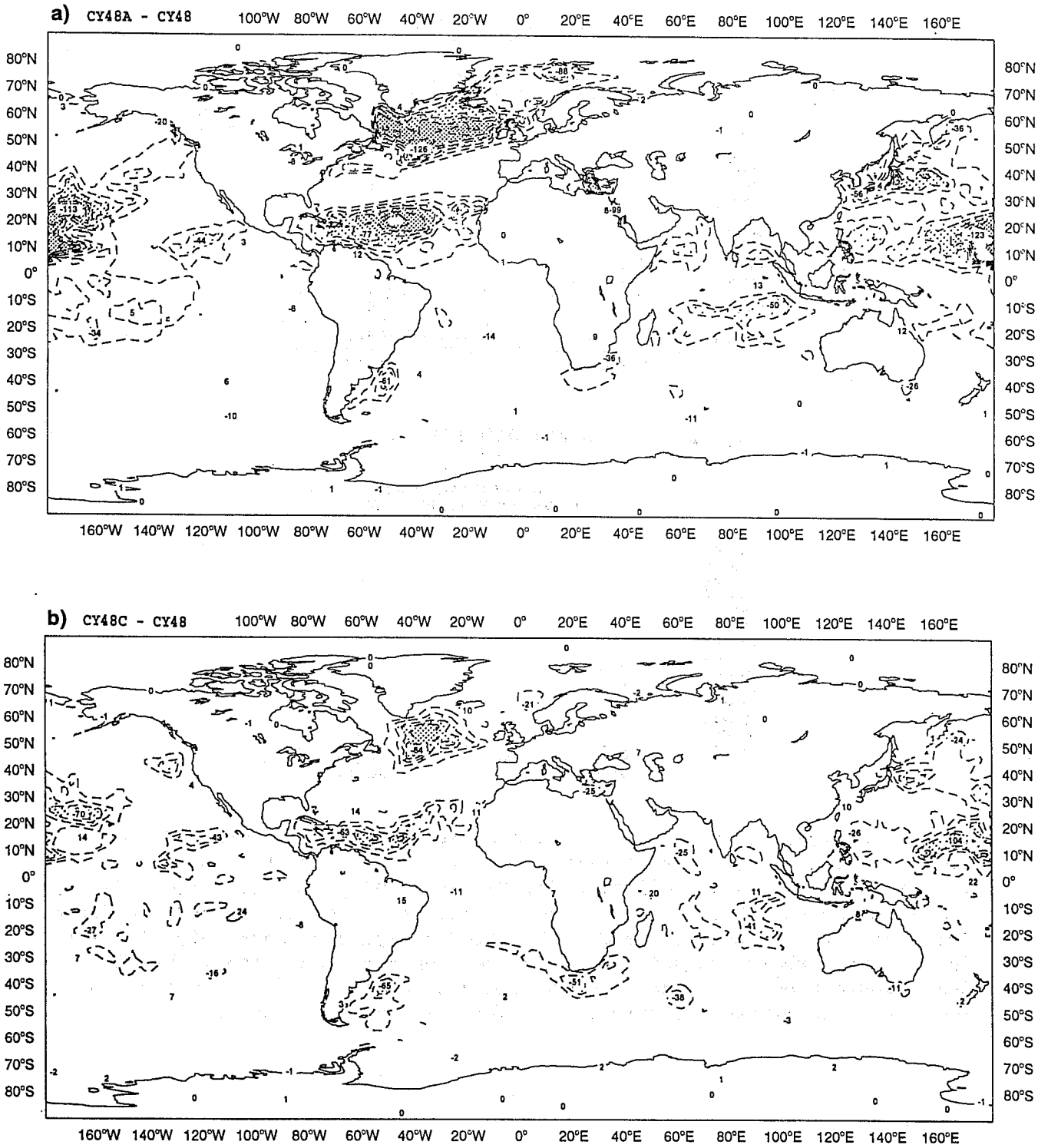

Fig. 9 Impact of enhanced air-sea interaction on latent heat flux (A) and the impact of revised closure in shallow convection on surface latent heat flux (B). These are differences of 24 hour accumulated values averaged over 5 forecasts from a data assimilation experiment (January 1993).

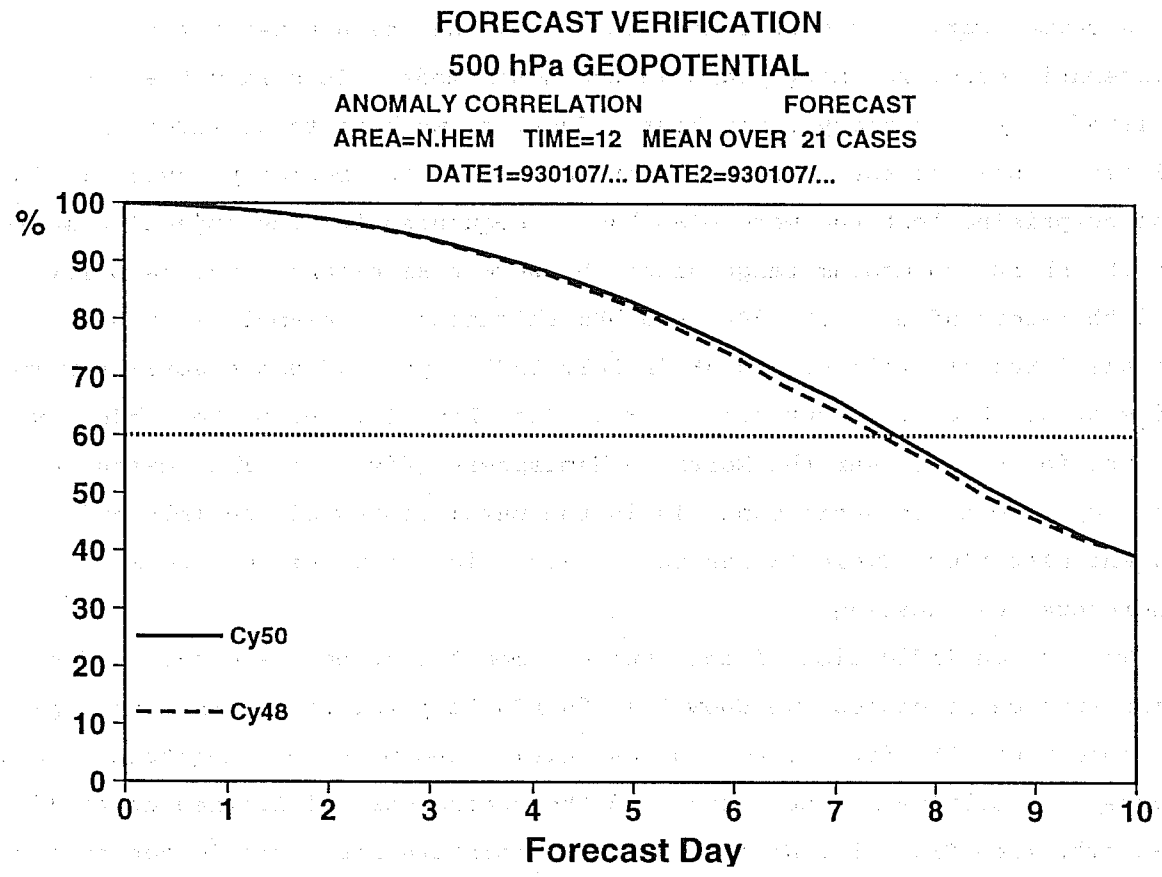

Fig. 10 Anomaly correlation for Northern Hemisphere averaged over 21 T106L31 forecasts from a data assimilation/forecast experiment. The dashed line is for cycle 48 and the solid line is for cycle 50 which has the revised closure for shallow convection as its main ingredient (January 1993).

3.1 Warm bias and entrainment

A summer warm bias over continental areas has been a persistent systematic error for many years in the ECMWF model. This warm bias is related to the boundary layer heat budget, so we have to consider the fluxes of heat at the surface and at the top of the boundary layer. It is not surprising that the warm bias has consequences for the objective scores in the short and medium range since the warm bias extends over deep layers and therefore affects the 500-1000 hPa thickness. An example is the parallel run of cycle 47 and 48 in July 1993: cycle 48 has a smaller warm bias at 850 hPa over continental areas (see Fig. 11) and better objective scores for summer over the Northern Hemisphere (Fig. 12). The reason for the improvement for this month is in the partitioning of sensible and latent heat flux. Cycle 48 has more evaporation from the surface and therefore less heating.

To give an indication of the type of impact that can be obtained from land surface processes, we show the 850 hPa temperature errors from a pair of long runs. The first long run was initialized with soil moisture from a rather dry multiyear integration and the second was initialized at field capacity (see Fig. 13). We see that soil moisture has a big impact on the warm bias, by making the soil more moist, the heating is reduced even on a seasonal time scale.

For comparison, we also show the impact from entrainment at the boundary layer top. For this purpose we use a pair of long runs and look again at the 850 hPa temperature error (Fig. 14). The first long run uses the boundary layer scheme with an explicit entrainment parametrization (see Beljaars and Betts, 1993). It uses a profile of diffusion coefficients in the mixed layer (without counter-gradient term) according to Troen and Mahrt (1986) and a buoyancy flux across the capping inversion which is 20 % of the surface buoyancy flux. The second long run uses the Louis et al. (1982) scheme which does not have entrainment. We see that the entrainment at the top of the boundary layer causes some heating, but the impact is much smaller than that from soil moisture. In fact the heating as caused by the entrainment parametrization makes the warm bias worse in the ECMWF model in spite of being physically more realistic. One of the reasons is

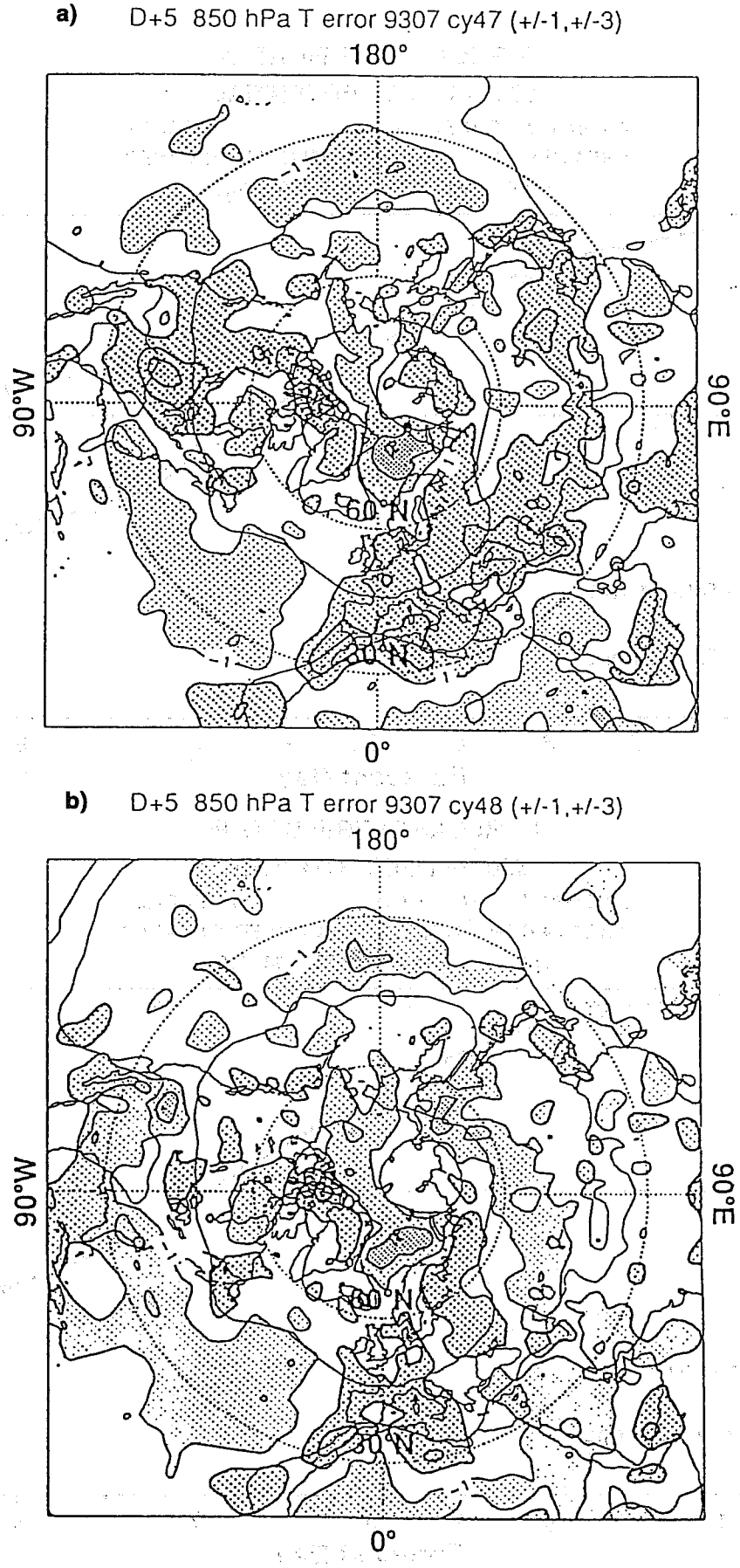

Fig. 11 Temperature error at 850 hPa of day five forecasts from 2 to 27 July 1993 for the operational suite with cycle 47 (A) and the parallel suite with cycle 48 (B).

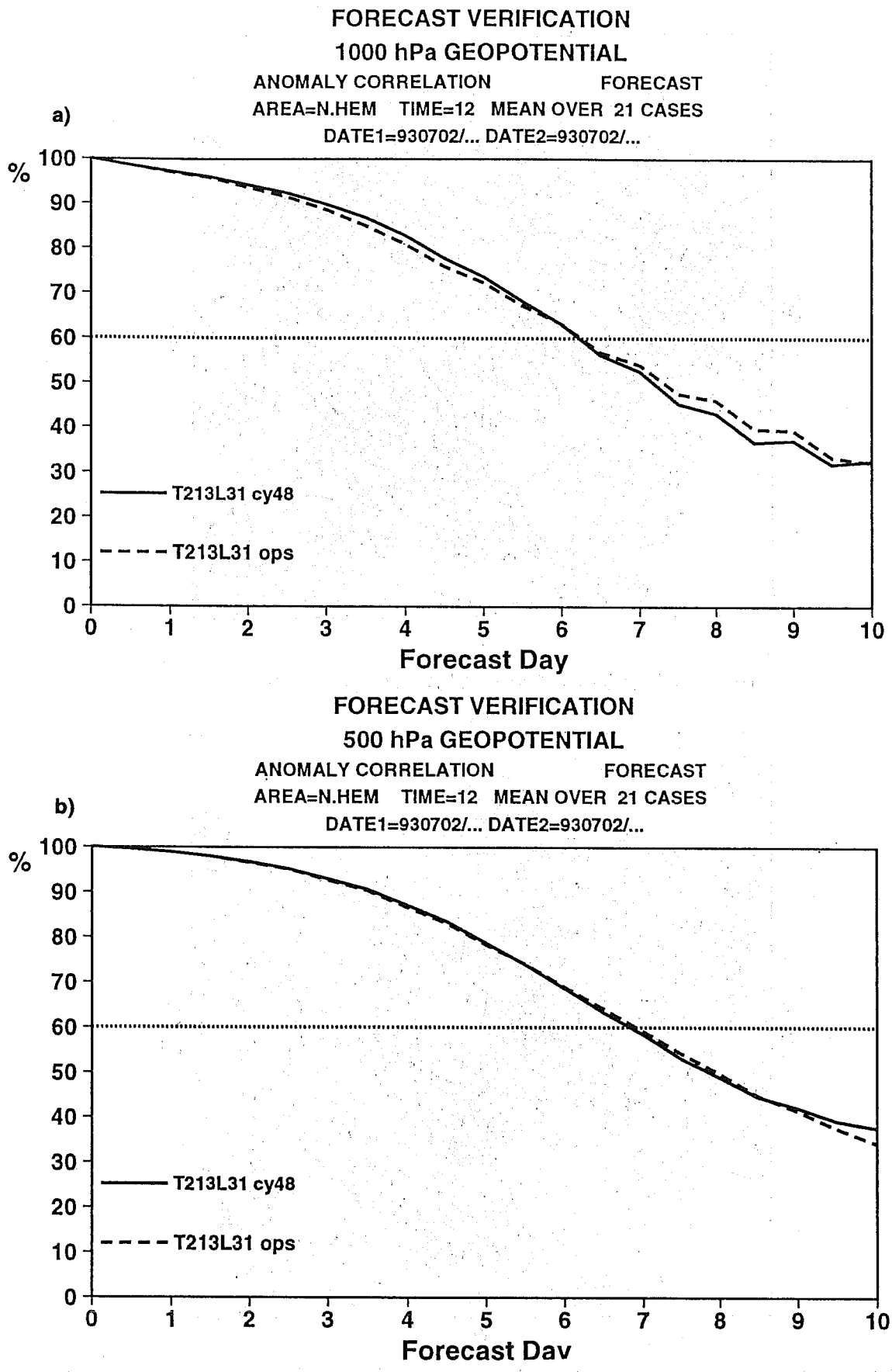

Fig. 12 Anomaly correlation for the N.Hemisphere at 1000 (A) and 500 hPa (B) averaged from 2 to 27 July 1993 from operational forecasts with cycle 47 (dashed) and the parallel suite with cycle 48 (solid).

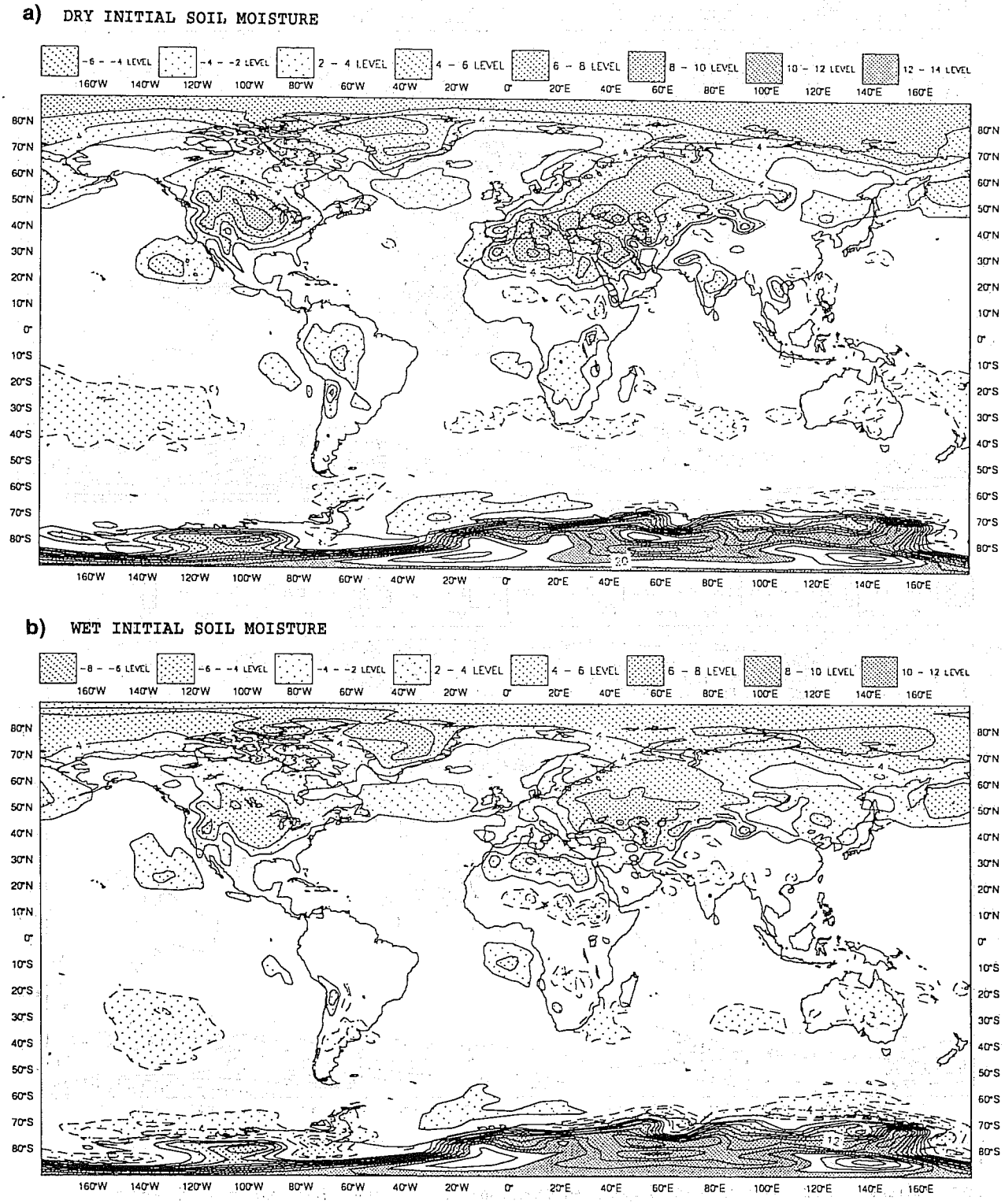

Fig. 13 Temperature errors of two long integrations starting from 1 May 1992 averaged over June-July-August. The soil moisture has been initialized from a multiyear integration (A; rather dry)) and at field capacity (B).

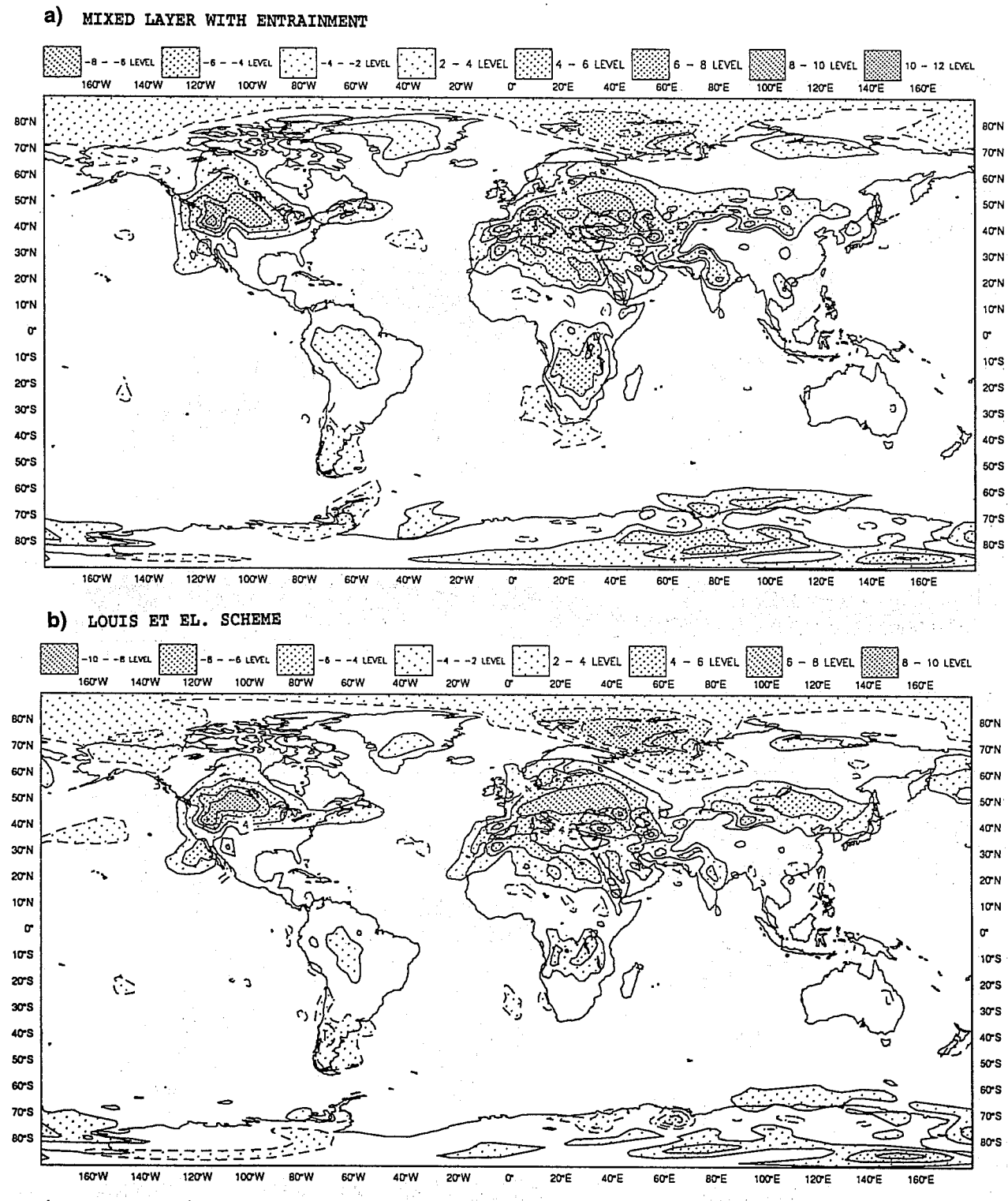

Fig. 14 As Fig 13 but from 1 April 1993 also averaged over June-July-August. Two different boundary layer parametrizations have been used here: the scheme with dry mixed layer entrainment (A ;see Beljaars and Betts, 1991) and the Louis et al. (1981) scheme (B).

the underestimation of cloud cover and overestimation of net radiation at the surface as seen in many models (e.g. Garratt et al., 1993; Garratt, 1994). The beneficial effect of entrainment is mainly seen in the short range in the boundary layer height and the near surface specific humidity. This is illustrated in the Figs. 15 and 16 with help of FIFE data. The scheme with entrainment produces a deeper and dryer boundary layer, which is more consistent with data.

From the examples above we conclude that the land surface energy budget is the dominant factor in the day time mixed layer temperature. The latter has considerable impact on the 1000-500 hPa thickness and consequently on the model performance in the medium range. The entrainment at the top of the boundary layer is the second important factor in determining the mixed layer heat budget. Entrainment has also a pronounced effect on the boundary layer moisture structure and on the boundary layer depth.

3.3 Diurnal cycle

Boundary layer parameters as temperature and specific humidity at screen level are important forecast products and are closely linked to the boundary layer parametrization and to the surface energy budget. Fig. 17 shows the operational verification of these parameters against SYNOP data for July 1993 with model cycle 47 and also with model cycle 48 which was running in parallel at that time. We see that the specific humidity has improved considerably with model cycle 48. This is the combined effect of increased moisture supply from the surface and increased drying through the boundary layer top. The day time temperature is also improved (lowered) with model cycle 48, but the night time temperature is worse with cycle 48. The reason is the overestimation of the amplitude of the diurnal temperature cycle which is virtually the same with both model cycles. This overestimation is related to the night time cooling.

Too get more insight in the characteristics of the diurnal temperature cycle, we look at the surface energy balance and near surface temperatures for Cabauw in The Netherlands where we have observations from a 200 m tower. Comparisons of different components of the surface energy balance,

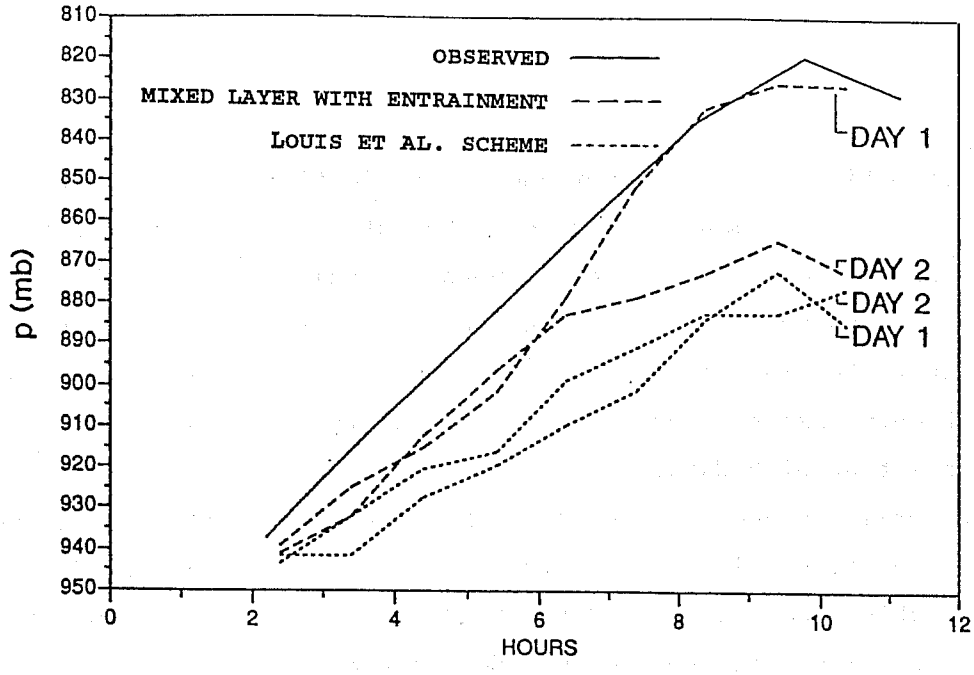

Fig. 15 Boundary layer development during day 1 and day 2 averaged over 9 forecasts in August 1987 in comparison with sonde data from the FIFE experiment (Beljaars and Betts, 1991). The solid line represents the data, the dashed line is with the boundary layer scheme with entrainment and the dotted line is with the Louis scheme. The horizontal scale is in hours counted from 12 UTC (start of the forecast or start of day 2 of the forecast), which is about 6 am local time.

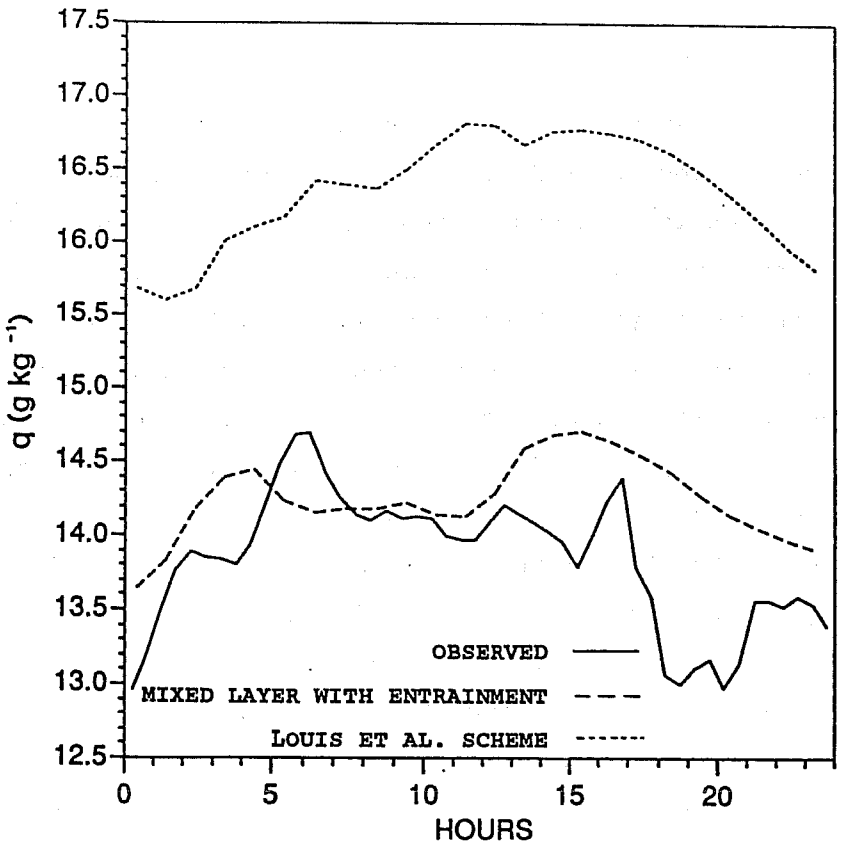

Fig. 16 As Fig. 15 for specific humidity during day one of 9 forecasts in August 1987 in comparison with FIFE data. The solid line represents the data, the dashed line is with the boundary layer scheme with entrainment and the dotted line is with the Louis scheme.

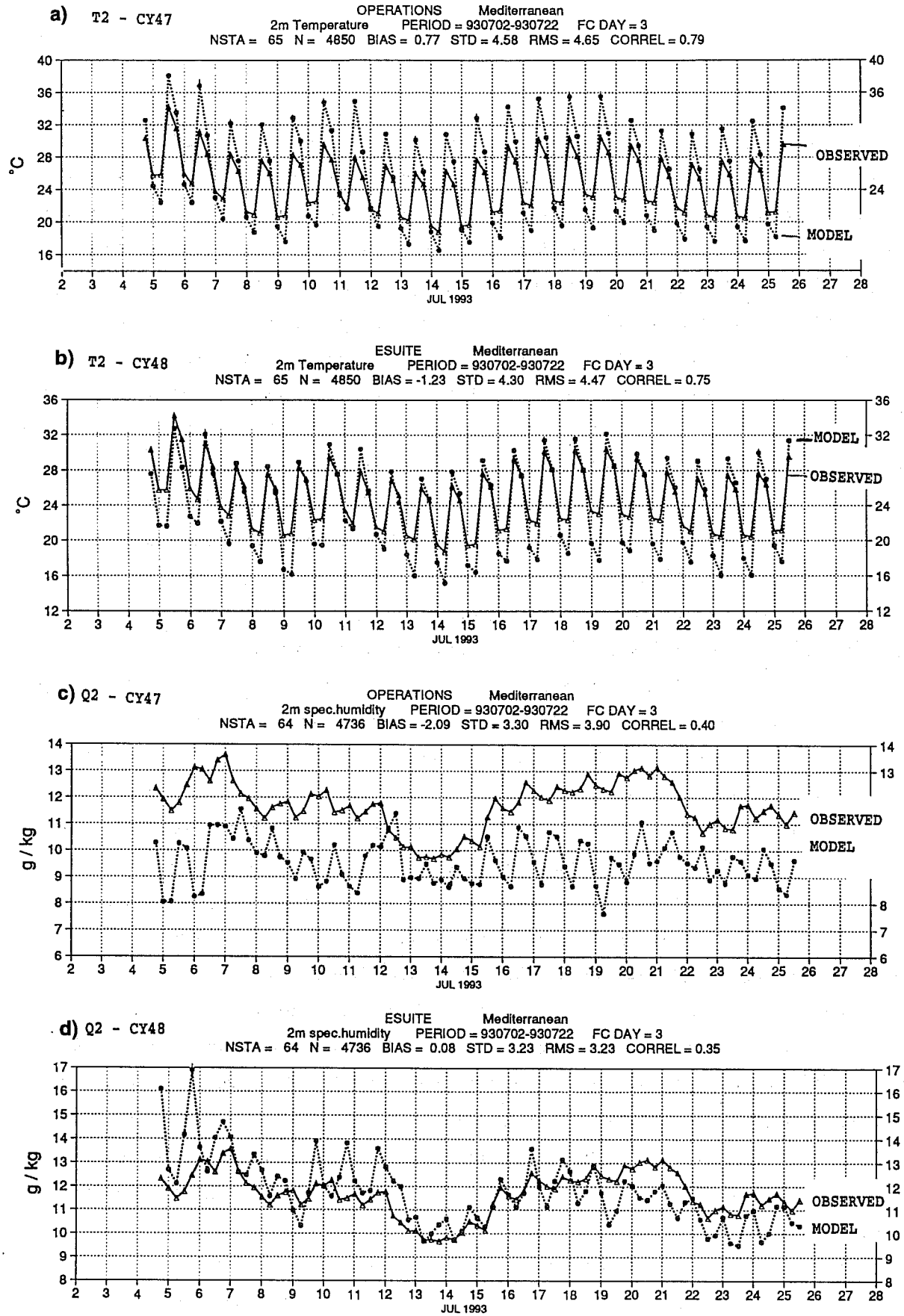

Fig. 17 Comparison of 54,60,66 and 72 hour forecasts of 2m temperature (A,B) and specific humidity (C,D) with data from all SYNOP stations in the Mediterranean area. Figs. (A,C) are for the operational model (cycle 47) between 5 and 25 July 1993, the Figs. (B,D) are from the parallel run with model cycle 48.

of temperatures and wind below 200 m are shown in the Figs. 18-21. We compare 6 hour averages of the forecasts up to day 1 with a time series of observed 30 minute averages (Fig. 18). First of all we notice that cooling by thermal radiation in the model is rather realistic in clear nights at a level of about 80 W/m2, but that in cloudy situations (e.g. day 325,326,331,332) the model largely overestimates the long wave cooling. Also the sensible heat flux looks realistic in comparison with observations. However, the downward latent heat fluxes (positive numbers) are rather low in the model. It is not clear how realistic the observed dew deposition fluxes are since they have been determined as a residual of the surface energy balance. The downward "observed" latent heat fluxes are actually larger than can be expected from theoretical considerations (see Garratt and Segal, 1988).

The diurnal evolution of the temperatures up to 200 m are shown in Fig. 19. The divergence between skin temperature, 2 m temperature and the temperature at the lowest model level is captured rather well by the model. Days with low wind (e.g. day 330) have a large gradient near the surface, whereas other days (e.g. day 329) have small gradients (see Fig. 21 for wind). The main difference between model and observations is the amplitude of the diurnal cycle near the surface and the amount of decoupling between levels 30 and 31. The night time temperature drop is too large in the model and the coupling between model level 30 and 31 is too weak. The latter is particularly true for the period between day 326 and 332, where the lowest model level is completely decoupled from the layer aloft.

Finally we show the ground heat flux from observations and from the model in Fig. 20. We see that the observed ground heat flux is typically 20 W/m^2, with a decrease to nearly 0 during day time. The ground heat fluxes in the model ar much higher, typically of the order of 50 W/m^2 during the night. This implies that the coupling of the atmosphere with the underlying soil is not the origin of the unrealistic temperature drop, but rather the result.

From this section we conclude that the model produces too low temperatures during the night. The underestimation of cloud cover or the underestimation of the effects of clouds is one of the problems. For the November 1993 period in Cabauw, the lack of vertical diffusion is probably

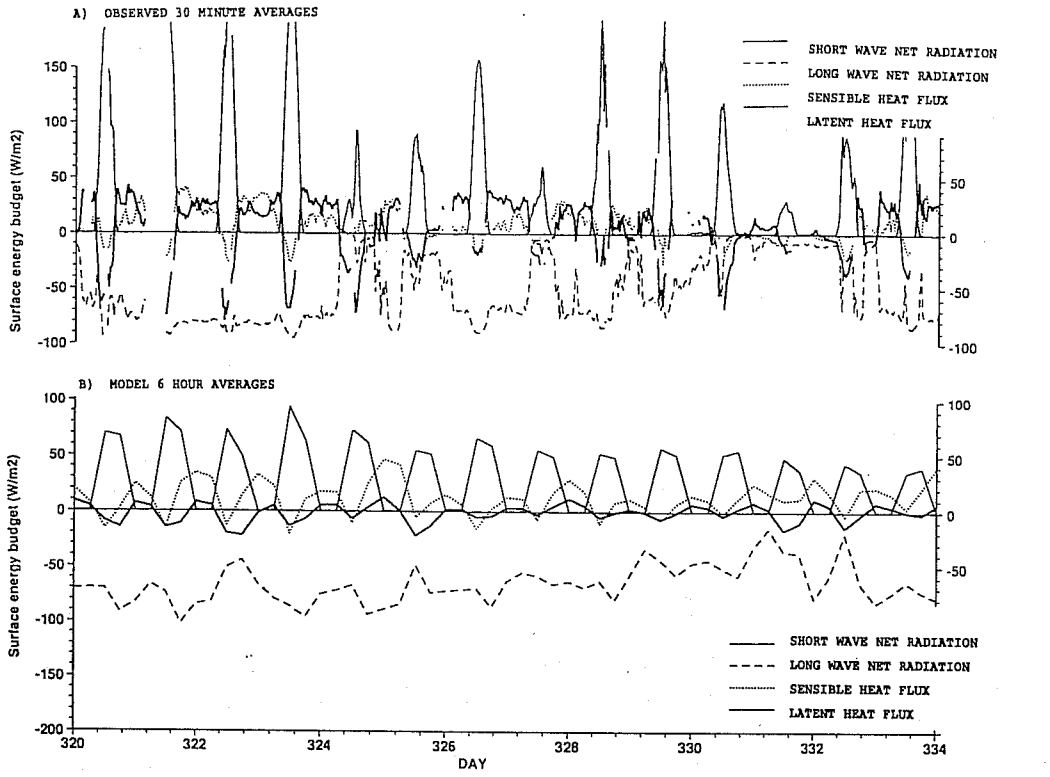

Fig. 18 Surface energy budget at Cabauw in The Netherlands for the second half of November 1993. Fig. (A) shows observed 30 min averages, the lower panel shows 6 hour averages of the operational forecasts from 0 to 6, 6 to 12, 12 to 18 and from 18 to 24 hours for successive days. The horizontal axis is the verifying day number.

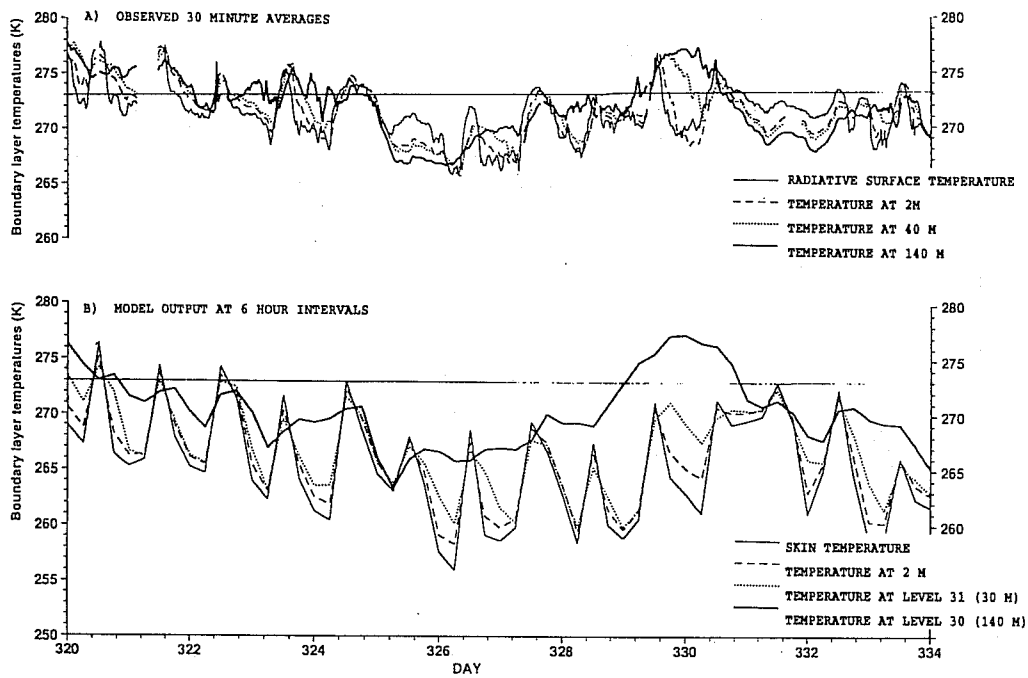

Fig. 19 Boundary layer temperatures at Cabauw in The Netherlands for the second half of November 1993. Fig. (A) shows observed 30 minute averages of the skin temperature (radiative surface temperature), the 2 m, 40 m and 140 m temperatures. Fig. (B) shows the 6, 12, 18 and 24 hour forecasts from successive days of the skin temperature, the 2 m, the level 31 (30 m) and the level 30 (140 m) temperatures.

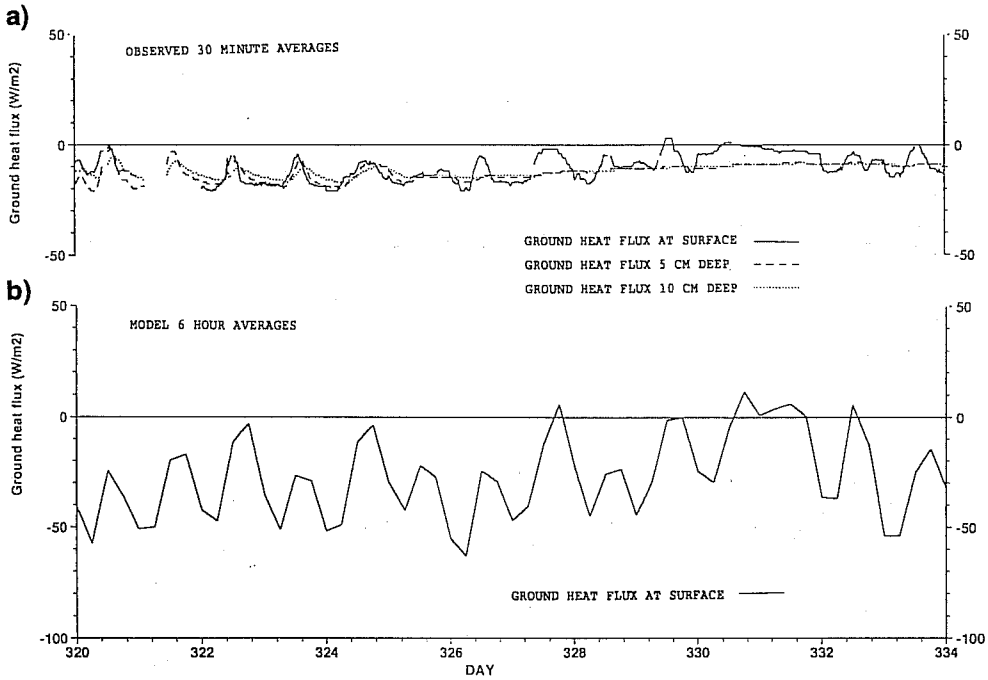

Fig. 20 Ground heat fluxes at Cabauw in The Netherlands for the second half of November 1993. Fig. (A) shows observed 30 minute averages of the ground heat flux at depths of 0, 5 and 10 cm. Fig. (B) shows the 6 hour averages of the ground heat flux at the surface of the operational forecasts from 0 to 6, from 6 to 12, from 12 to 18 and from 18 to 24 hours for successive days.

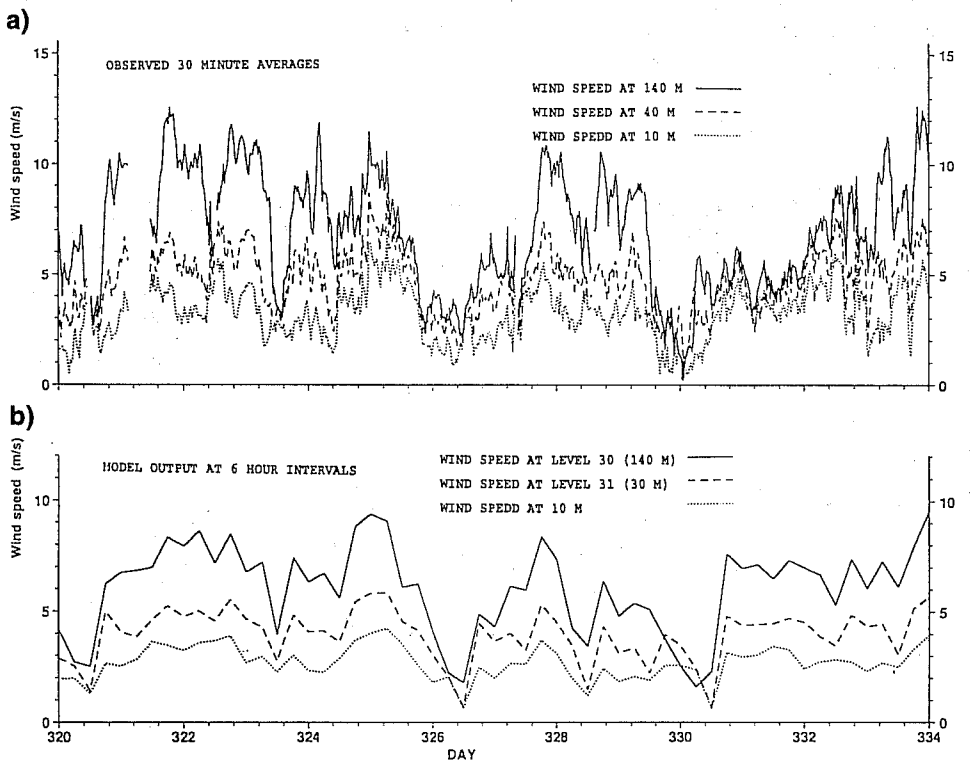

Fig. 21 Wind at Cabauw in The Netherlands for the second half of November 1993. Fig. (A) shows observed 30 minute averages of wind speeds at heights of 10, 40 and 140 m. Fig. (B) shows the 6, 12, 18 and 24 hour forecasts of successive days of wind speeds at 10m, level 31 (30 m) and level 30 (140 m).

the dominant cause of the night time negative temperature bias. The reason for this is not very clear, but the stability functions play obviously a central role. Experimentation with the stability functions proposed by Beljaars and Holtslag (1991) showed an improvement. The stability function for heat is virtually the same as the one by Louis et al. (1982) but the one for momentum is much lower leading to more shear and therefore to higher diffusion of heat (see next section for discussion of stability functions). However, it is also very well possible that current parametrizations miss a fundamental mechanism which enhances the turbulent diffusion. Examples are subgrid katabatic effects, mesoscale meandering of the flow and terrain heterogeneities.

4. Momentum fluxes over land

The momentum budget of the atmosphere is an extremely complicated issue since it involves the turbulent surface stress, the subgrid wave stress and the orographic resolved drag. A discussion of the global momentum budget is beyond the scope of this paper (see e.g. Peixoto and Oort, 1992); here we limit to an example of sensitivity. Aspects of mountain torque and gravity wave drag are discussed by Palmer et al. (1986), Wallace et al. (1983) and Miller et al. (1989).

Observations of momentum exchange with the earth surface are very difficult and nonexistent on a routine basis. Therefore compensating errors can easily remain unnoticed. For example, turbulent surface drag and mountain drag (gravity wave drag and resolved drag) may be both deficient and compensate each other in many situations.

Here we will discuss turbulent surface drag over land only and try to use as much as possible the knowledge of boundary layer processes as obtained from field experiments. Two aspects have to be distinguished when considering turbulent surface drag: (i) the specification of the surface roughness length and (ii) the diffusion of momentum in the boundary layer. The surface roughness length has to include effects of subgrid orography, which are parametrized in the ECMWF model following the ideas developed by Mason (1991). However, such parametrizations rely heavily on the slope of

the subgrid orography and the current global data sets are inadequate to derive such a slope parameter. In practice it is very difficult to assess the quality of the resulting turbulent orographic drag since data on this process only exists for very few locations during short periods of time.

With regard to boundary layer diffusion, the situation is different. The magnitude of the turbulent diffusion in the boundary layer has been a popular topic in boundary layer research for many years (see e.g. Stull, 1988; Garratt, 1992). The eddy diffusivities can be related to Monin Obhukov stability functions for the surface layer on the basis of similarity theory. Following the idea of local scaling proposed by Nieuwstadt (1984, see also Derbyshire, 1990) these functions should also apply to the stable boundary layer above the surface layer. The unstable boundary layer is different since the eddy diffusivity concept breaks down and the eddies have dimensions of the order of the boundary layer depth with a strong nonlocal character. However, the strong mixing in the unstable boundary layer results in a very simple structure, namely a well mixed layer. So, even here the eddy diffusivity works reasonably well, as long as the diffusion is strong enough to keep the mixed layer well mixed. Also effects of entrainment and contergradient transport can be added in reasonably simple ways (e.g. Beljaars and Betts, 1993; Holtslag and Moeng, 1991; Holtslag and Boville, 1993).

We now consider the impact of the stability functions in stable situations. The functions that are in use in the operational ECMWF model for stable situations are the ones proposed by Louis et al. (1982). These functions are not based on experimental data but on considerations of asymptotic behavior and to a certain degree inspired by model performance. In Fig. 22 we compare the Louis functions with functions derived from Monin Obukhov stability functions (Beljaars and Holtslag, 1991). The latter are based on a reasonable consensus of experimental data (see Högström, 1988 for a review). It is clear from Fig. 22 that the Louis functions lead to overestimation of the turbulent diffusion, particularly of the momentum diffusion. This is also illustrated by the one column simulations shown in Fig. 23. For a geostrophic wind of 10 m/s over land with a surface roughness length of 0.1 m, the Louis functions produce an equilibrium boundary layer depth of about 600 m, whereas the M.O. formulation results

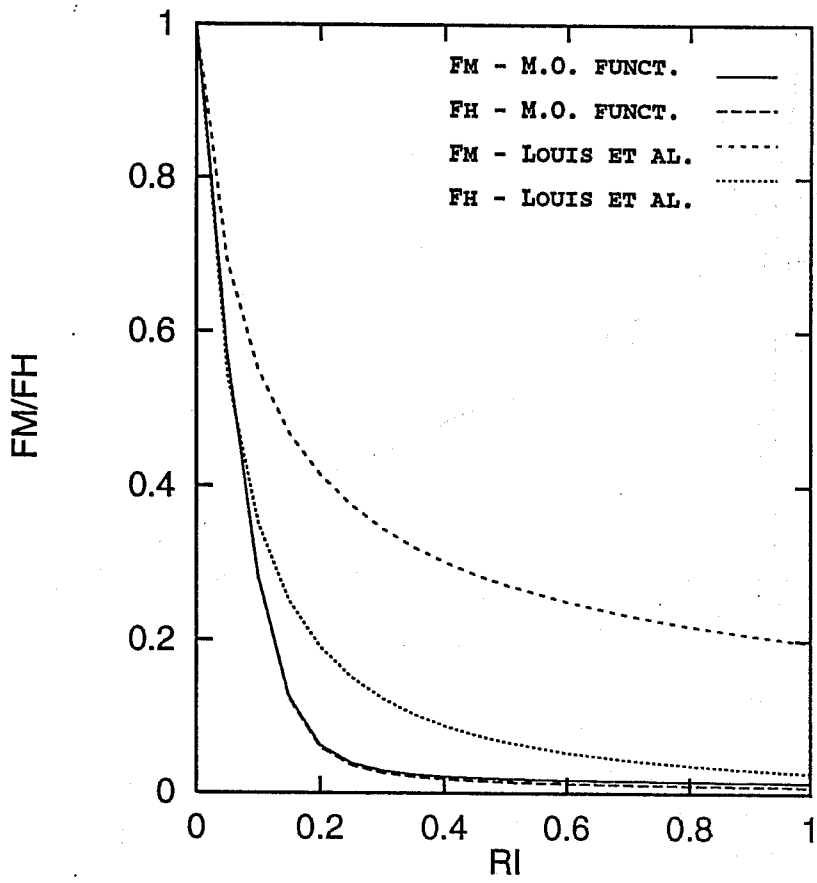

Fig. 22 Stability functions in the eddy diffusivity formulation of the Louis (1979) scheme for momentum (Fm) and heat/moisture (Fh) for stable situations. The formulation as operational in the ECMWF model (Louis et al., 1982) is compared with the one derived from Monin Obukhov similarity (Beljaars and Holtslag, 1991).

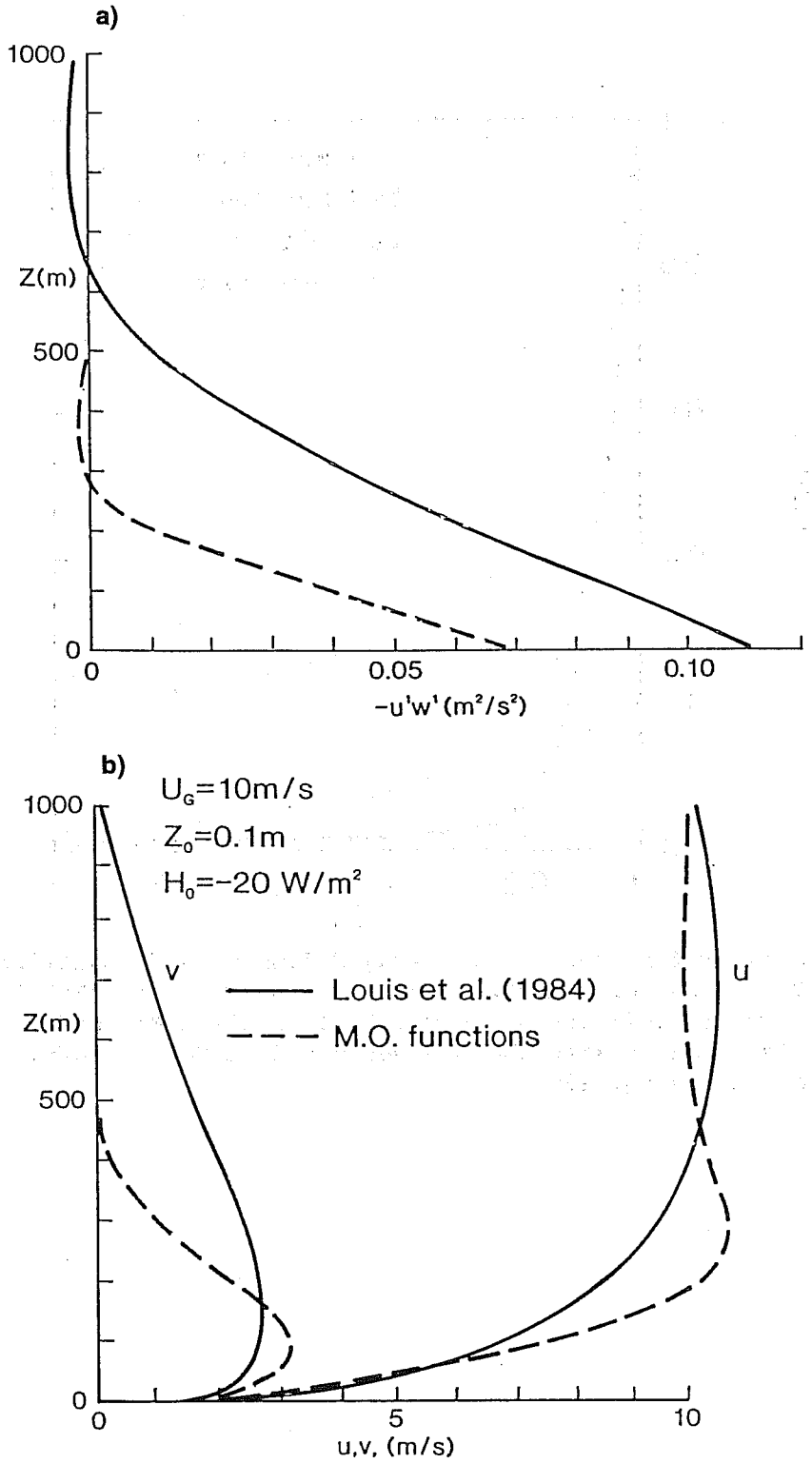

Fig. 23 One column simulation of stress (A) and wind (B) in the stable boundary layer after 9 hours of integration with the Louis et al. (1982) stability functions and the ones derived from M.O. similarity. The geostrophic wind is 10 m/s in the x-direction and constant in time and height. The surface roughness length is 0.1 m and a constant downward heat flux of 20 W/m^2 is applied at the surface.

in a boundary layer of about 200 m. Observations and empirical formulae support the value of about 200 m (Zilitinkevich, 1972; Nieuwstadt, 1981). One could argue that the vertical resolution of the model is inadequate to represent such shallow layers near the surface. However, in a one column resolution study by Beljaars (1992) it is shown that poor resolution as in the ECMWF model does not dramatically deteriorate the simulation of the stable boundary layer. Another illustration of the difference between the Louis functions and the M.O. functions is the geostrophic drag law computed from one column simulations. The results are presented in Fig. 24 with help of the parameters A and B as a function of the dimensional stability parameter (see e.g. Stull, 1988 for the definition of A and B). The M.O. functions produce a more realistic drag law in comparison with Wangara data (Clarke and Hess, 1974), with less friction and a larger a-geostrophic angle than the Louis functions.

Also results from the ECMWF model in the past have given a clear indication of overestimation of vertical diffusion in stable situations. When the scheme is applied throughout the model atmosphere it leads to considerable smearing of the jet stream, which is particularly detrimental to the data assimilation system. This was the reason to switch off the scheme above a generous estimate of the boundary layer depth. Another signal from the model is the amplitude of the diurnal cycle of temperature as shown in section 3.3. Replacement of the Louis functions by the M.O. functions alleviates this problem.

The evidence on the deficiencies of the stability functions has never been sufficient for an operational change, The reason is illustrated in Fig. 25: The change from the Louis functions to the M.O. functions leads to a deterioration of the model performance over the Northern Hemisphere especially for winter. The reason is not very clear at this moment. It is known from sensitivity experiments that the detrimental impact is coming from land areas and that it is most likely related to the reduction of surface drag. It is also known that the reduced vertical diffusion with the M.O. functions result in a higher level of eddy kinetic energy in the model.

The increase of eddy kinetic energy might be interpreted as lack of Ekman damping. To get a qualitative impression of the Ekman damping in the

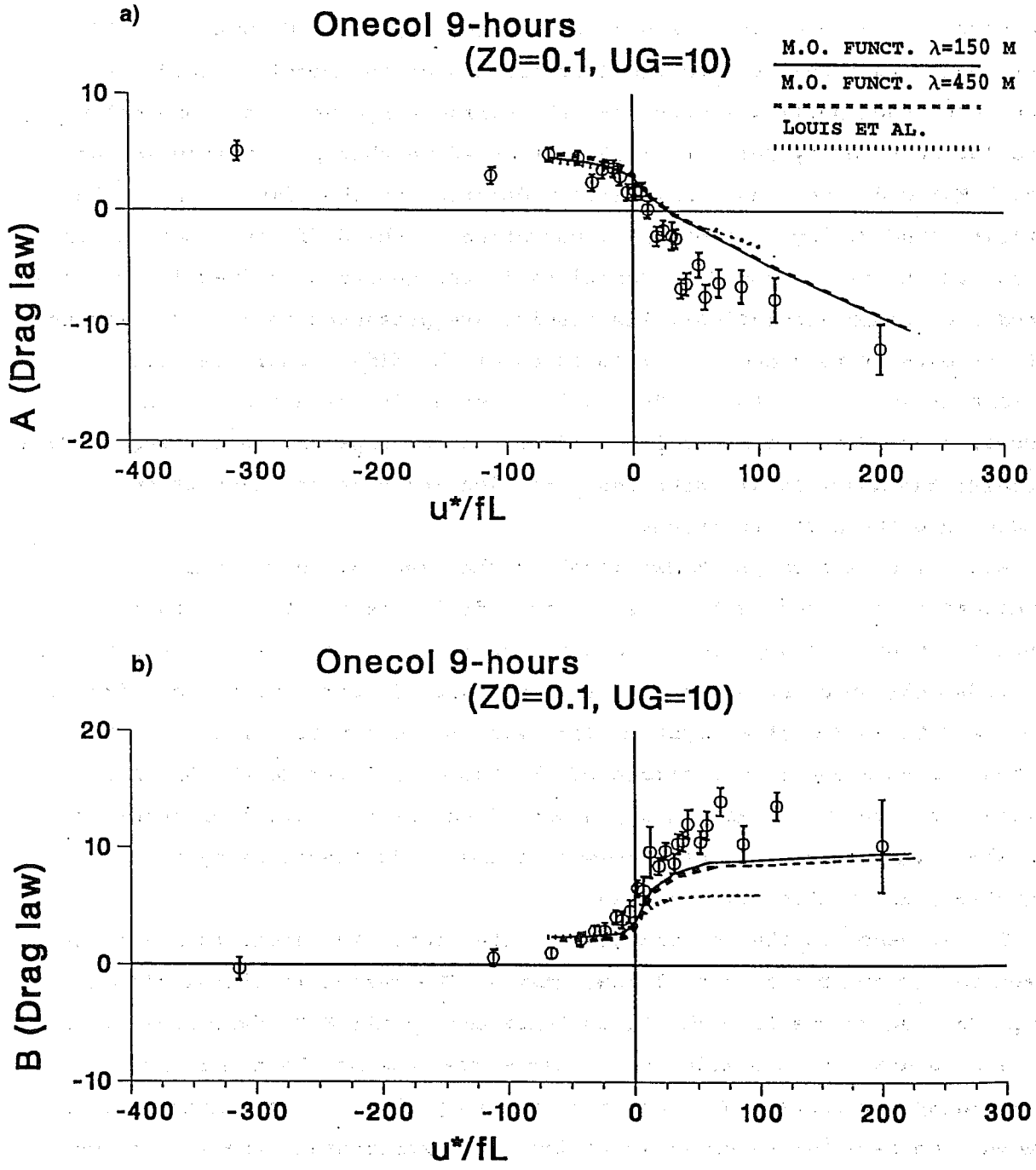

Fig. 24 Parameters A and B in the geostrophic drag law (see e.g. Stull, 1988) as a function of stability from one column simulations in comparison with Wangara data (Clarke and Hess, 1974). The stability functions derived from M.O. similarity are compared with the ones proposed by Louis et al. (1982). Also two asymptotic mixing lengths are compared. Parameter A is indicative for the surface drag, parameter B for the a-geostrophic angle. Higher values of A and B imply more drag and a larger a-geostrophic angle respectively. The parameter on the horizontal axis is a stability parameter based on friction velocity u*, Coriolis parameter f and Obukhov length L.

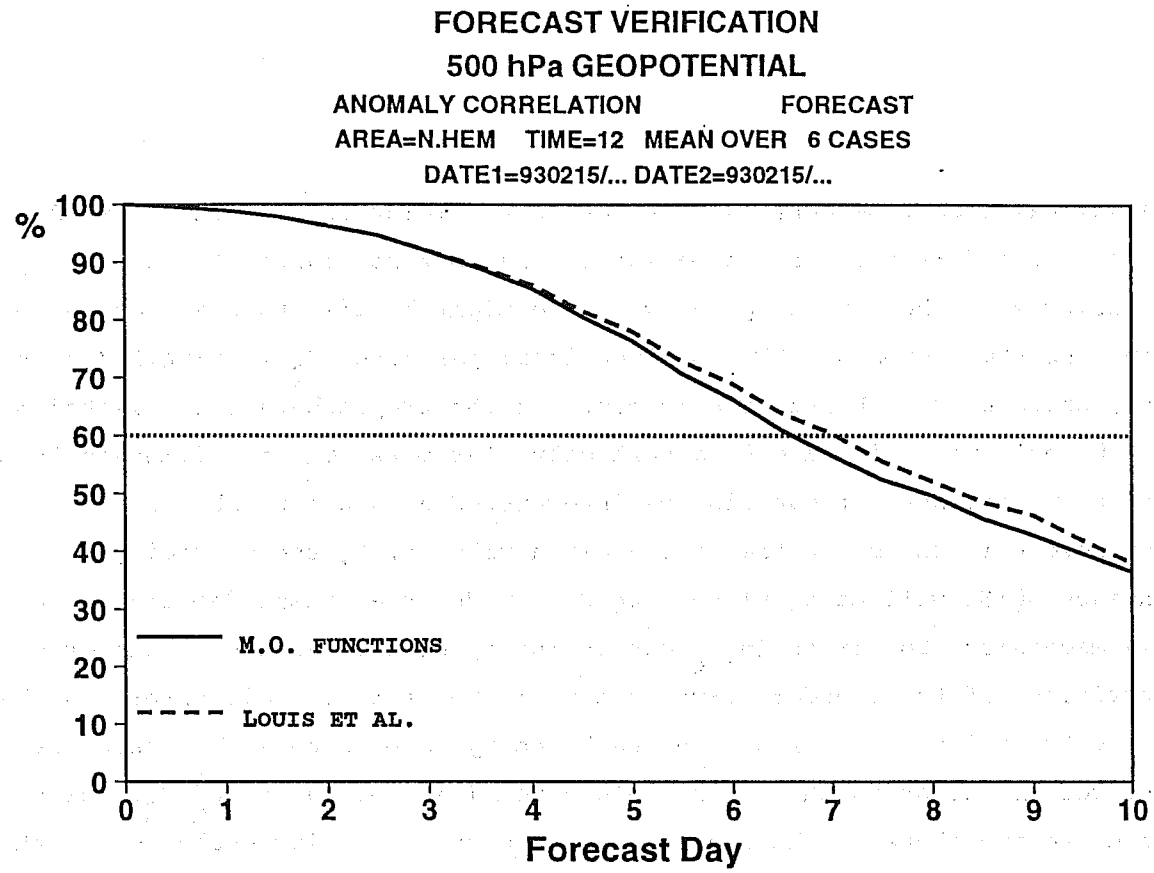

Fig. 25 Anomaly correlation for the Northern Hemisphere at 500 hPa averaged over 6 forecasts with the Louis et al. (1982) stability functions and the functions derived from M.O. similarity.

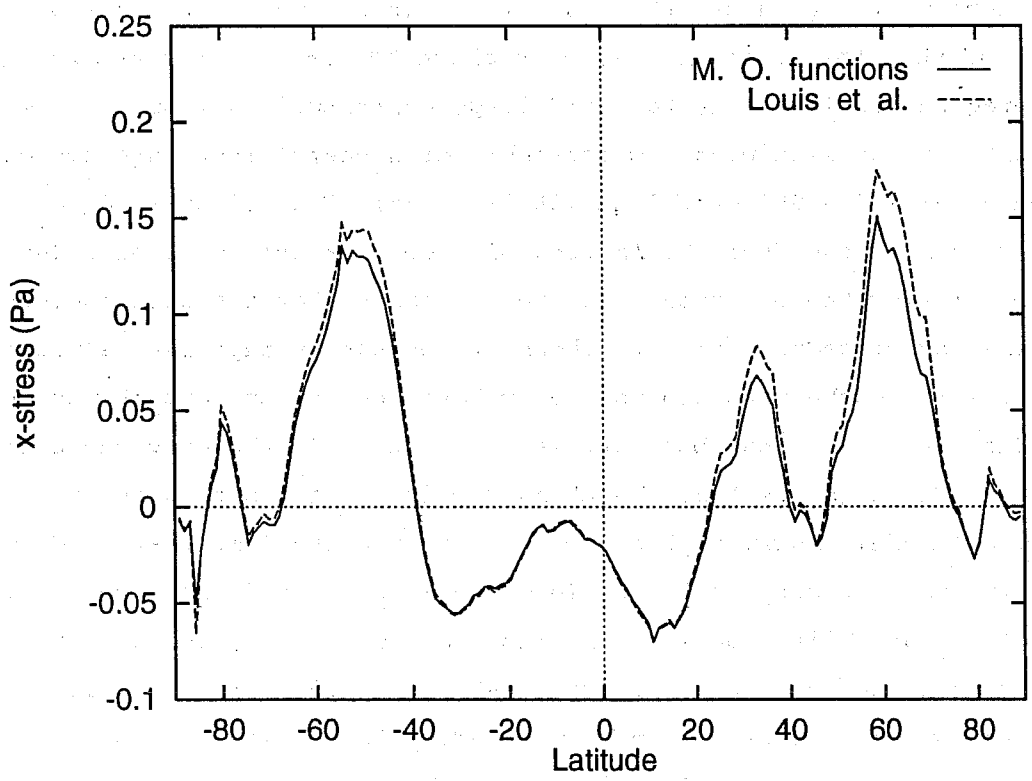

Fig. 26 Zonal turbulent surface stress zonally averaged and averaged over a 72 hours forecast with the Louis et al. scheme and with the stability functions derived from M.O. similarity.

operational model, we consider the vorticity evolution over the first 24 hours of the forecasts. By comparing the 24 hour forecasts of cyclonic vorticity with the verifying analysis, we might be able to draw conclusions about the Ekman damping. The nondimensional parameter $C_\zeta = (D/U\zeta)\partial\zeta/\partial t$ is used, where D is a characteristic depth of the troposphere (we selected 5 km), U horizontal wind and ζ is vorticity. Parameter C_ζ is a dimensionless vorticity tendency. It can also be interpreted as a geostrophic drag coefficient in the sense that for a given value of C_ζ the vorticity tendency $\partial\zeta/\partial t$ will be equal to $C_\zeta U\zeta/D$ provided that Ekman damping is the only mechanism. So errors in C_ζ can be interpreted as errors in the drag coefficient of the boundary layer scheme if we attribute all errors in the vorticity evolution to errors in the boundary layer scheme. We therefore consider the error in the dimensionless vorticity evolution $C_\zeta^f - C_\zeta^a$, which is the difference between the coefficient from the vorticity evolution of the forecast and that of the analysis. In this way we obtain an error from the vorticity evolution and interpret it as an error in the geostrophic drag coefficient. To reduce the noise in the results we also apply averaging over a number of days under the condition that the vorticity is above $10^{-5}s^{-1}$ and that the horizontal wind is above 10 m/s. It is necessary to do the averaging conditionally to avoid large contributions from areas with weak vorticity or weak winds. Geostrophic drag coefficients are typically between 0.001 and 0.002 over land (Stull, 1988). Fig. 27 shows $C_\zeta^f - C_\zeta^a$ averaged over 12 days over N. America with contour intervals of 0.005. The lower panel show the percentage of the forecasts that has been included in the averaging procedure. Fig. 27 shows predominantly negative values also over areas where the wind and vorticity have been strong enough most of the time. When we assume that boundary layer friction is the only cause for the error in C_ζ it suggests that the Ekman damping is too strong in the operational model. However, there may be other mechanisms that lead to errors in the vorticity evolution (e.g. horizontal diffusion) so it is difficult to draw firm conclusions. The least we can say is that the diagnostics of the vorticity evolution above the boundary layer is not in conflict with what we have seen from boundary layer similarity studies namely: the boundary layer friction is too high.

Since the modification of the stability function has impact on the

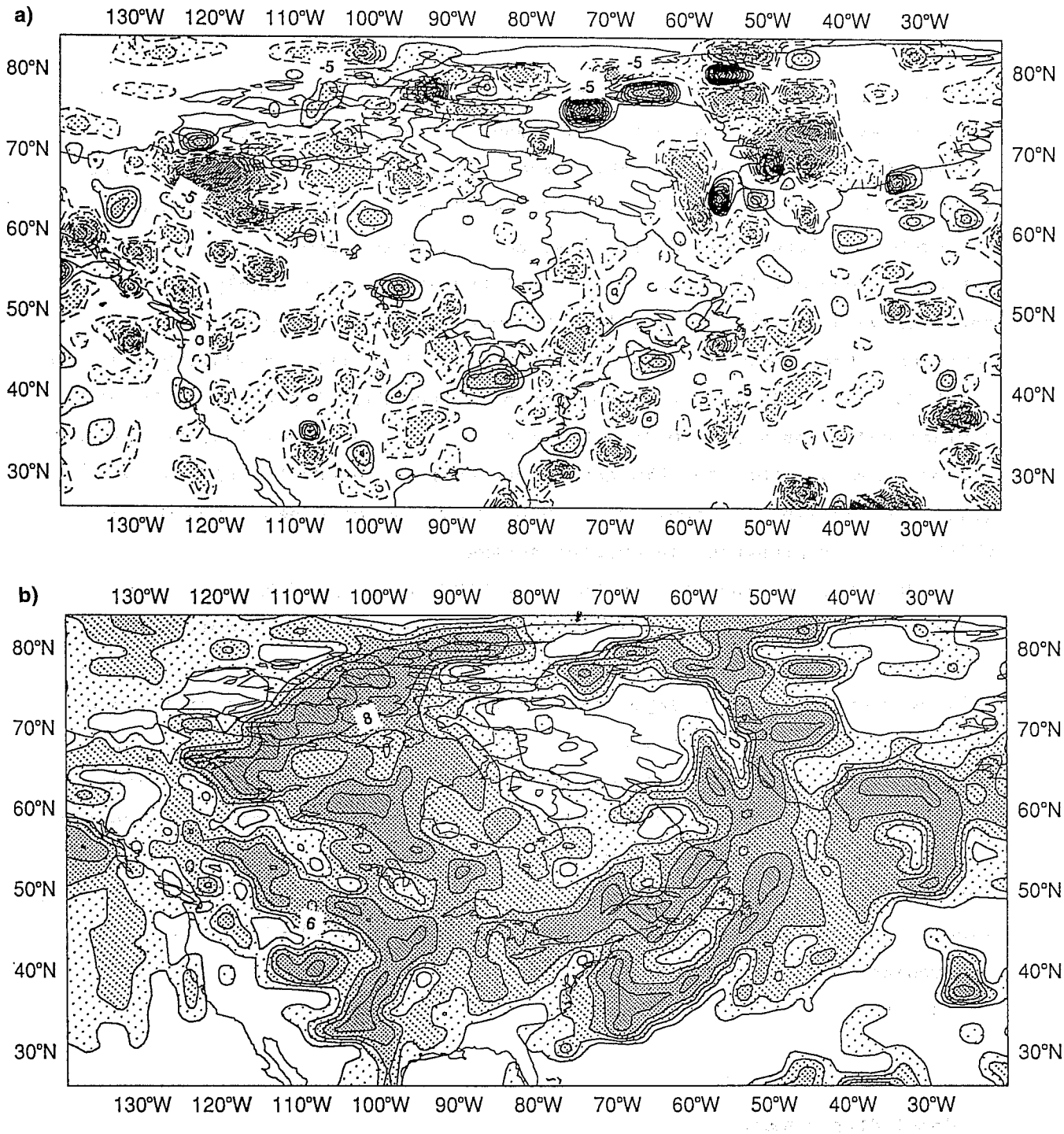

Fig. 27 (A): Difference between dimensionless vorticity evolution in forecast C_ζ^f and analysis C_ζ^a, where $C_\zeta = (D/U\zeta)\partial\zeta/\partial t$. The difference is directly computed by taking the difference between 24 hour forecasts of vorticity and the analysis and scaling with $(D/U\zeta)/\partial t$, where D is 5 km and ∂t is 24 hours. Vorticity is taken from level 26 (850 hPa) and the result is averaged over 12 forecasts under the condition that U > 10 m/s and that $\zeta > 10^{-5}$ s^{-1}. The contour interval is 0.0005. Dashed contours represent negative values.
(B) The percentage of forecasts that has been included in the average. The contour interval is 20 %.

medium range performance rather than on the short range, there might be a relation with the angular momentum budget. To get some quantitative information on the impact of the stability functions we show the surface stress zonally averaged and averaged over 72 hours of a forecast with the two stability functions. It is clear that the M.O. functions produce less surface stress and the deterioration of the scores is probably related to this. If we adopt the hypothesis that some drag is missing with the M.O. functions, then there is a range of possibilities: (i) the gravity wave drag might be too small, (ii) the interaction of boundary layer stability with surface roughness may be poorly represented (for roughness lengths that are not much smaller than the Obukhov length current theory is inadequate), (iii) interaction of turbulence with orography might enhance the mixing which is not represented in current schemes.

We draw the conclusion here that the ECMWF model performance is very sensitive to the parametrization of momentum diffusion in stable situations. The current parametrization does not reflect the results from well documented boundary layer experiments over flat homogeneous terrain, but are rather inspired by model performance. This may be due to compensating errors. The current parametrization for stably stratified turbulent diffusion was introduced before the schemes for gravity wave drag and momentum flux by convection. The latter may be compensating for deficiencies in the boundary layer scheme. It is also possible that essential mechanisms are missing. Examples are: subgrid effects of heterogeneous terrain and katabatic flow over sloping terrain in stable situations.

5. Concluding remarks

A number of examples has been given of model sensitivity to changes in the boundary layer formulation of the ECMWF model. The main conclusion is that impact in the medium range is often related to changes in the surface fluxes. Impact from changes to evaporation from the ocean has been demonstrated for low winds in the tropics and for strong winds in the extratropics. Changes to the surface fluxes are not necessarily related to

the surface flux parametrization itself. Also ventilation at the top of the boundary layer causes enhanced surface evaporation. So the entire boundary layer structure is important for the parametrization of surface fluxes and particularly the interaction with other processes e.g. convection. The latter has been illustrated for a winter situation with cold air outflow over the western Atlantic.

The surface fluxes of heat and moisture over land are of considerable importance to the temperature and moisture structure over deep layers in the lower troposphere. As such they affect the pressure fields and need to be considered carefully for medium range forecasting. The surface fluxes are of primary importance, but entrainment at the top of the boundary layer plays an important role as well. The latter is noticeable in temperature (entrainment causes heating), but is even more pronounced in moisture (entrainment causes drying).

The diurnal cycle near the surface is closely related to the boundary layer parametrization. We have seen that the amplitude of the diurnal cycle in temperature is too large in the operational ECMWF model, mainly caused by too much night time cooling. The unrealistic stability functions are partly responsible for this, but also underestimation of cloud cover and perhaps missing mixing mechanisms as katabatic flow, meso-scale activity and terrain heterogeneity may play a role.

The parametrization of the surface momentum flux is probably the most sensitive aspect of boundary layer parametrization, when considering model performance in the medium range. The current parametrization with the Louis functions has deficiencies that can be documented from different points of view. However, the high level of surface drag produced by this parametrization is beneficial to the model performance for reasons that are not very clear at this moment. There are many possible causes ranging from compensating errors (e.g. compensation between gravity wave drag, turbulent drag and resolved mountain drag), interaction of stratified turbulence with orography to missing mechanisms as subgrid katabatic flow, mesoscale variability and terrain heterogeneity.

Research in the area of stably stratified near surface flow should have high priority since it is important for general circulation models and it is hindering further development in boundary layer parametrization. For

instance, introduction of more advanced schemes (e.g. higher order closure) is difficult since it implies a more realistic stable boundary layer with lower drag than the current Louis scheme. This would automatically lead to a deterioration of the model performance which is not acceptable for an operational model.

Acknowledgement

I would like to thank Bert Holtslag, Martin Miller and Aad van Ulden for their constructive comments on an early version of the manuscript.

Literature

Beljaars, A.C.M. and Holtslag, A.A.M. (1991): On flux parametrization over land surfaces for atmospheric models, J. Appl. Meteor., 30, 327-341.

Beljaars, A.C.M. (1992): Numerical schemes for parametrizations, ECMWF Seminar proceedings 9-13 September 1991, Numerical methods in atmospheric models, Vol II, 1-42.

Beljaars, A.C.M. and Betts, A.K. (1993): Validation of the boundary layer scheme in the ECMWF model, ECMWF Seminar proceedings 7-11 September 1992, Validation of models over Europe, Vol II, .

Beljaars, A.C.M. (1995): The parametrization of surface fluxes in large scale models under free convection, Quart. J. Roy. Meteor. Soc., in press

Bradley, E.F., Coppin, P.A. and Godfrey, J.S. (1991): Measurements of sensible and latent heat fluxes in the western equatorial pacific ocean, J. Geoph. Res., 96, Suppl. 3375-3389.

Clarke, R.H. and Hess, G.D. (1974): Geostrophic departure and the functions A and B of Rossby-number theory, Bound.-Layer Meteor., 7, 267-287.

DeCosmo, J. (1991): Air-sea exchange of momentum heat and water vapor over whitecap sea states, PhD thesis, Univ. of Washington, Seattle, 212 pp.

Derbyshire, S.H. (1990): Nieuwstadt's SBL revisited, Quart. J. Roy. Meteor. Soc., 116, 127-158.

Garratt, J.R. and Segal, M. (1988): On the contribution of atmospheric moisture to dew formation, Bound.-Layer Meteor., 45, 209-236.

Garratt, J.R. (1992): The atmospheric boundary layer, Cambridge University Press, 316 pp.

Garratt, J.R. (1993): Sensitivity of climate simulations to land-surface and atmospheric boundary-layer treatments- A review, J. Clim., 6, 419-449.

Garratt, J.R., Krummel, P.B. and Kowalczyk, E.A. (1993): The surface energy balance at local and regional scales- A comparison of general circulation model results with observations, J. Clim., 6, 1090-1109.

Garratt, J.R. (1994): Incoming shortwave fluxes at the surface - A

comparison of GCM results with observations, J. Clim., 7, 72-80.
Högström, U. (1988): Non-dimensional wind and temperature profiles in the atmospheric surface layer: A re-evaluation, Bound.-Layer Meteor., 42, 55-78.
Holtslag, A.A.M. and Moeng, C.H. (1991): On eddy diffusivity and counter-gradient transport in the convective atmospheric boundary layer, J. Atmos. Sci., 48, 1690-1698.
Holtslag, A.A.M. and Boville, B.A. (1993): Local versus nonlocal boundary-layer diffusion in a global climate model, J. Clim., 1825-1842.
Liu, W.T., Katsaros, K.B. and Businger, J.A. (1979): Bulk parameterization of air-sea exchange of heat and water vapor including the molecular constraints at the interface, J. Atmos. Sci., 36, 1722-1735.
Louis, J.F. (1979): A parametric model of vertical eddy fluxes in the atmosphere, Bound.-Layer Meteor., 17, 187-202.
Louis, J.F., Tiedtke, M. and Geleyn, J.F. (1982): A short history of the operational PBL-parameterization at ECMWF, Workshop on boundary layer parameterization, November 1981, ECMWF, Reading, England.
Mason, P.J. (1991): Boundary layer parametrization in heterogeneous terrain, In: ECMWF workshop proceedings on Fine-scale modelling and the development of parametrization schemes.
Miller, M.J., Palmer, T.N. and Swinbank, R. (1989): Parametrization and influence of subgrid orography in general circulation and numerical weather prediction models, Meteor. Atmos. Phys., 40, 84-109.
Miller, M., Beljaars, A.C.M. and Palmer, T.N. (1992): The sensitivity of the ECMWF model to the parametrization of evaporation from the tropical oceans, J. Clim., 5, 418-434.
Nieuwstadt, F.T.M. (1981): The steady-state height and resistance laws of the nocturnal boundary layer: Theory compared with Cabauw observations, Bound.-Layer Meteor., 20, 3-17.
Nieuwstadt, F.T.M. (1984): The turbulent structure of the stable, nocturnal boundary layer, J. Atmos. Sci., 41, 2202-2216.
Palmer, T.N.G., Shutts, G.J. and Swinbank, R. (1986): Alleviation of a systematic Westerly bias in general circulation and numerical weather prediction models through an orographic gravity wave parameterization, Quart. J. Roy. Meteor. Soc., 112, 1001-1039.
Peixoto, J.P. and Oort, A.H. (1992): Physics of climate, Am. Inst. Phys., New York, 520 pp.
Schumann, U. (1988): Minimum friction velocity and heat transfer in the rough surface layer of a convective boundary layer , Bound.-Layer Meteor., 44, 311-326.
Stull, R.B. (1988): An introduction to boundary layer meteorology, Kluwer Acad. Publ., Boston, 666 pp.
Tiedtke, M., Heckley, W.A. and Slingo, J. (1988): Tropical forecasting at ECMWF: The influence of physical parameterization on the mean structure of forecasts and analysis, Quart. J. Roy. Meteor. Soc., 114, 639-664.
Troen, I. and Mahrt, L. (1986): A simple model of the atmospheric boundary layer; sensitivity to surface evaporation, Bound.-Layer Meteor., 37, 129-148.
Wallace, J.M., Tibaldi, S. and Simmons, A.J. (1983): Reduction of systematic errors in the ECMWF model through the introduction of an envelope orography, Quart. J. Roy. Meteor. Soc., 109, 683-717.
Zilitinkevich, S.S. (1972): On the determination of the height of the Ekman boundary layer, Bound.-Layer Meteor., 3, 141-145.